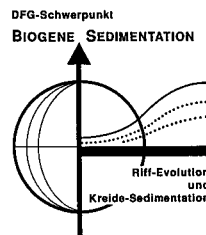
	Festschrift zum 60. Geburtstag von Erik Flügel			Redaktion: Baba Senowbari-Daryan & Albert Daurer	
	Abh. Geol. B.-A.	ISSN 0378-0864 ISBN 3-900312-90-7	Band 50	S. 31-56	Wien, 6. April 1994

Attempted Reconstruction of Permian and Triassic Skeletonization from Reefbuilders (Oman, Turkey): Quantitative Assessment with Digital Image Analysis

By MICHAELA BERNECKER & OLIVER WEIDLICH*)

With 5 Text-Figures, 8 Tables and 6 Plates



Oman
Türkei
Perm
Trias
Tethys
Riffbildner
Skelettstärke
Digitale Bildanalyse

Contents

Zusammenfassung	31
Abstract	32
1. Introduction	32
2. Method	32
2.1. Description of the Method	32
2.2. Problems of Data Evaluation	33
3. Material and Study Areas	33
4. Data of Upper Permian and Upper Triassic Reefbuilders	35
4.1. "Sphinctozoans"	35
4.1.1. Upper Permian "Sphinctozoans"	35
4.1.2. Upper Triassic "Sphinctozoans"	37
4.2. Inozoans	37
4.2.1. Upper Permian Inozoans	38
4.2.2. Upper Triassic Inozoans	38
4.3. Chaetetids and Hydrozoans	38
4.3.1. Upper Permian Chaetetids	38
4.3.2. Upper Triassic Chaetetids	39
4.3.3. Problematical Upper Permian Hydrozoans	39
4.3.4. Upper Triassic Hydrozoans	39
4.4. Upper Permian Rugose Corals	40
4.5. Upper Triassic Scleractinians	40
5. Interpretation	41
5.1. Discussion of Data	41
5.2. Discussion of Reefbuilders	42
5.3. Application of Quantitative Skeleton Data: Recognition of Reefbuilding Guild Attribution	43
5.4. Ancient Versus Modern Skeletal Density: An Attempted Comparison	44
6. So, What Potential Does this Technique Have?	44
Acknowledgements	44
References	56

Versuch einer Rekonstruktion der Skelettstärke bei permischen und triassischen Riffbildnern (Oman, Türkei): Eine quantitative Untersuchung mit Hilfe digitaler Bildanalyse

Zusammenfassung

Die Skelettbildung (in Flächen-%) und die Masse des Skeletts (in g/cm³) wurden an oberpermischen und obertriassischen Riffbildnern von verschiedenen Lokalitäten aus dem Oman und der Türkei quantitativ untersucht. Zur Datenerhebung mit Hilfe der digitalen Bildanalyse „Vidas“ wurden Dünnschliffe verwendet. Die quantitativen Daten werden mit Taxonomie, Morphologie und Mikrofazies in Relation gesetzt, um den Einfluß der Diagenese und die Unterschiede in der Größe und Orientierung im Dünnschliff zu berücksichtigen. Die untersuchten Skelette zeigen eine deutliche Bandbreite von gut erhalten bis rekristallisiert mit Reliktstrukturen.

*) Anschrift der Verfasser: MICHAELA BERNECKER, Institut für Paläontologie, Universität Erlangen-Nürnberg, Loewenichstraße 28, D-91054 Erlangen; OLIVER WEIDLICH, TU Berlin, Institut für Geologie und Paläontologie, Sekr. EB 10, Ernst-Reuter-Platz 1, D-10587 Berlin.

Die untersuchten Gerüstbildner sind Sphinctozoen, Inozoen, Chaetetiden, rugose Korallen, Scleractinier und Hydrozoen. Die gemessenen Parameter können sowohl bei höheren Taxa (z.B. Skelett der Sphinctozoen 21–54 %) als auch auf Artniveau (Skelett von *Alpinothalamia bavarica* 29–51 %) deutlich variieren. Die Variation ist auf drei Hauptfaktoren zurückzuführen:

- a) unterschiedliche Morphotypen,
- b) intraspezifische Variabilität und
- c) Variation der Skelettelemente innerhalb einer Kolonie.

Mit quantitativen Parametern lassen sich stark und schwach verkalkte Taxa voneinander abgrenzen und ermöglichen eine objektive Zuordnung im Guild-Konzept von FAGERSTRÖM (1987).

Quantitative Messungen der Skelettstärke und der Masse des Skelettes liefern wichtige Daten für die Diskussion über Paläoproduktivität der Riffbildner und die Sedimentbilanz von fossilen Riffen.

Abstract

Upper Permian and Upper Triassic reefbuilders from different tectonic units of the Oman Mountains and Turkey were analyzed quantitatively with respect to skeletonization (skeleton in area percent) and skeletal mass (skeleton in g/cm³). Data were derived from thin-sections using the digital image analysis system 'Vidas'. The quantitative data were combined with taxonomy, description of gross morphology and microfacies analysis in order to understand the influences of diagenesis in the differing sizes and orientations of thin-sections. The investigated skeletons exhibit a wide range of preservation, ranging from unaltered to recrystallized with relic structures.

Reefbuilders studied were "sphinctozoans", "inozoans", "chaetetids", rugose corals, scleractinians, and hydrozoans. The measured parameters vary considerably for higher taxa (e.g., skeletonization of sphinctozoan sponges is 21–54 %) as well as for species (e.g., the skeletonization of the sphinctozoan *Alpinothalamia bavarica* is 29–51 %). The variation is regarded to be triggered by three main factors:

- a) differences in morphotypes,
- b) intraspecific variability, and
- c) variation of skeletal elements within the colony.

Well-skeletonized and weakly skeletonized higher taxa were observed in the mean skeletonization and the mean skeletal mass. These data help refine the guild concept proposed by FAGERSTRÖM (1987).

The quantitative assessment of the skeletonization and skeletal mass may provide data for the discussion about paleoproductivity of reefbuilders and the sedimentary net budget of ancient reefs.

1. Introduction

Reefbuilders of Upper Permian sponge/*Tubiphytes* reefs and Upper Triassic coral/sponge reefs have been analyzed with respect to taxonomy and paleoecology since the last century (cf. reef bibliography of FLÜGEL & FLÜGEL-KÄHLER, 1992). Common Upper Permian reefbuilders at higher taxonomic levels are "sphinctozoans", "inozoans", "chaetetids", hydrozoans, algae, problematical taxa (e.g. *Archaeolithoporella*, *Tubiphytes*, and *Lercaritubus*), bryozoans and crinoids. Permian rugose and tabulate corals are less frequent in reefs; they commonly occur in level bottoms. Upper Triassic reefs are characterized by scleractinians, chaetetids, spongiomorphids, hydrozoans, algae and numerous problematic taxa. There is no quantitative data on the skeletal mass secreted by these reefbuilders, despite their importance (FAGERSTRÖM, 1991).

This paper concentrates on the quantification of skeletonization as well as the skeletal mass of Late Paleozoic and Early Mesozoic reefbuilders. Utilizing digital image analysis via a PC, the degree of skeletonization can be measured in area percent without pointcounting. The method was tested for different groups and morphotypes of reefbuilding organisms (sphinctozoans, inozoans, chaetetids, hydrozoans, spongiomorphids, rugose corals, and scleractinians).

2. Method

2.1. Description of the Method

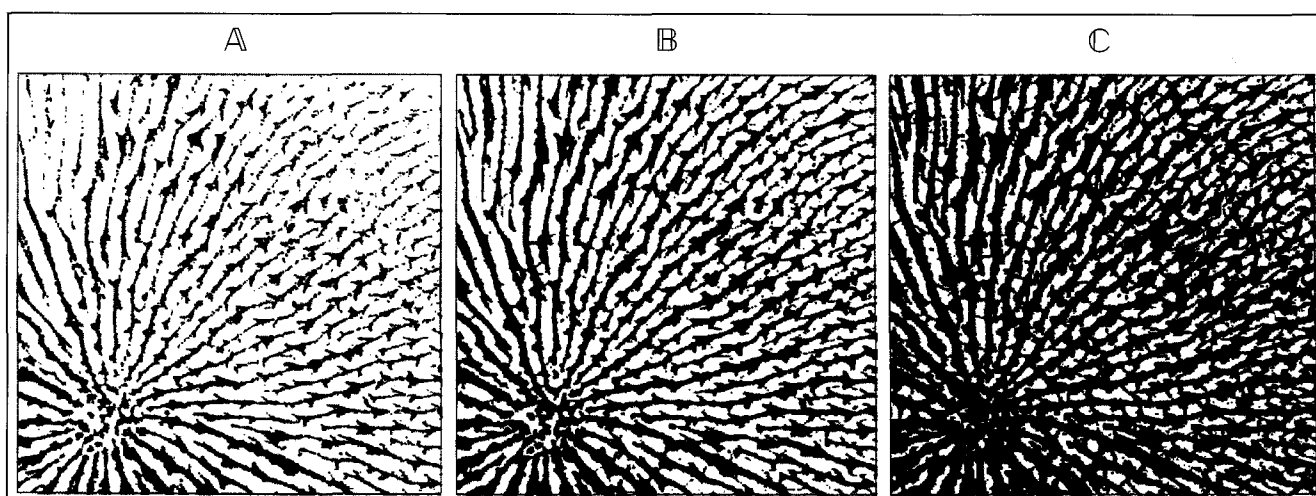
Calcification of modern reefbuilders can be calculated from X-radiographs exhibiting variations in X-ray film density due to skeletal banding. These data can be converted to coral bulk density (g/cm³). Measurement parameters characterizing the skeleton comprise the amount of CaCO₃ secreted in low or high density growth as well as

the annual mass accretion. The error of measurement is estimated to be 5 %. The method for data evaluation was described by BUDEMEIER (1974) and applied by DODGE & BRASS (1984). BOSSCHER (1992) used medical X-ray computerized tomography in the study of coral skeletons. Skeletal mass is calculated by both techniques in g/cm³.

More studies of the skeletonization than the fossil counterparts have been done on modern reefbuilders. FAGERSTRÖM (1987, 1991) described qualitatively higher modern and ancient reefbuilding taxa as well-skeletonized or less skeletonized.

The degree of skeletonization is not considered as an isolated criterion, but is related to taxonomy, gross morphology, and microfacies analysis in order to reconstruct the degree of primary skeletonization despite the diagenetic overprint. Gross morphology was studied in slabs; taxonomy, microfacies analysis and skeletonization from thin-sections. Thin-sections are considered best suited for the quantitative study of skeletonization, because cements and skeleton can be easily distinguished during measurement.

We used the digital image analysis system 'Vidas Kontron Image Analysis Division' coupled to a PC and Video Camera. The digital input consists of pictures made by a video camera. The image analysis system calculates in area percent the different grey values of the picture. The different grey values represent the skeleton and the cement or micrite. Reefbuilders surrounded by micrite with a distinct contrast between dark sediment and light skeleton permit direct measurements from video pictures. Recrystallized reefbuilders surrounded by cements may need to be manually outlined, owing to similar grey values. Cements and recrystallized skeleton cannot be differentiated by the computer. The data output of the image analysis system always consist of two elements:



Text-Fig. 1.
Discrimination of the skeleton of ancient reefbuilders correct or distorted.
(a) underestimation of the skeleton, (b) correct measurement, (c) overestimation of the skeleton (see Pl. 6/3,4).

- 1) skeletonization in area percent and
- 2) a laser print of the measured area, which is used for interpretation and control.

In addition, the volume of the skeleton is converted into skeletal mass to make the data comparable to those of modern reefbuilders.

2.2. Problems of Data Evaluation

Three main questions need to be clarified before skeletonization of fossil reefbuilders can be reconstructed.

■ Unaltered skeletal mineralogy versus diagenetic overprint

The best data are achieved from unaltered reefbuilders lacking diagenetic overprint. Excellent preservation is extremely rare; it is, however, described for Permian reefbuilders from Timor (SORAUF, 1982) and for Triassic reefbuilders from allochthonous boulders (Cipit boulders) of the Northern Calcareous Alps (e.g., Zlambach Beds, RONIEWICZ, 1989) and Turkey (Dereköy Unit, CUIF, 1972).

Unaltered material was analyzed in this paper, based only on Upper Triassic reefbuilders of the Cipit boulders, Turkey. The bulk of the investigated reefbuilders secreted metastable aragonitic skeletons. Exceptions comprise some Upper Triassic sphinctozoans composed of Mg-calcite (SENOWBARI-DARYAN, 1990) and rugose corals composed of Mg-calcite (e.g., SORAUF 1983) and/or aragonite (WENDT, 1990; OEKENTORP, 1980). The aragonitic skeletons have recrystallized to calcite, representing the common preservation of most Phanerozoic reefbuilders. Nevertheless, recrystallized skeletons may provide good data, if the intraparticle pores were filled with micrite prior to recrystallization. The sediment then preserves the unaltered primary skeletons.

Organisms without fine-grained sediment in their intrapores (e.g., reefbuilders constructed by closely stacked skeletal elements) are usually recrystallized and exhibit cemented intraparticle pores. Similar grey values of the skeletons and cement usually cause an overestimation of skeletal mass. Relic structures, such as the micrite envelopes often surrounding recrystallized skeletons, facilitate the differentiation of skeleton

and cement. Skeletonization in this case can be detected from detailed outline drawings of the reefbuilders in thin-sections in order to improve the data. In addition, reefbuilders need to be analyzed for marine phreatic cements surrounding the skeleton prior to an infill of the intraparticle pores. Strongly cemented reefbuilders lead to false data values which are too high for skeletonization. Totally recrystallized reefbuilders lacking any relic structures cannot be analyzed.

■ Size and orientation of thin-sections

In his morphometric analysis of Devonian stromatopores FAGERSTROM (1982) strongly emphasized a high level of intracoenosteal variation caused by: (1) small investigation areas (thin-section) and (2) different orientation of measured area (cross, longitudinal, and tangential sections). These parameters may also influence our data and must, therefore, be considered. Data calculation of higher taxa was carried out for both close-up views and larger areas. In addition, the type of thin-section was described for every measurement.

■ Measured data versus primary skeleton

Measurements of skeletonization always require careful data evaluation, because the decision of which grey values to measure and which to exclude may cause overestimation or underestimation of skeletal mass (Text-Fig. 1). To avoid misinterpretations, laser prints of equally grey areas of the measured skeleton can be compared with the thin-section in order to detect the accuracy of the measurement.

The brief description of possible difficulties suggests that application of microfacies analysis (FLÜGEL, 1982), carbonate petrography and knowledge about the calcification of organisms are necessary for the calculation of the skeletonization of ancient reefbuilders.

3. Material and Study Areas

The study comprises Upper Permian and Upper Triassic reefal organisms of the Oman Mountains (Text-Fig. 2) and Turkey (Text-Fig. 3).

① Upper Permian and Upper Triassic Reefbuilders of the Hawasina Nappes, Oman Mountains

The Hawasina nappes represent the relics of a former basin situated northeast of the Arabian platform, yield-

Text-Fig. 2.

Major geological units of the Oman Mountains.

Sample units are in the Sumeini Group (Jebel Wasa, 1) and the Hawasina nappes (Jebel Kaur, 2; area near Birkat al Mawz, 3; Ba'id area, 4).

ing enigmatic Upper Permian and Triassic carbonate klippen called "Oman Exotics" (GLENNIE et al., 1974). They are mainly of reefal and bedded platform facies. Subordinate slope deposits occur, too (SEARLE & GRAHAM 1982).

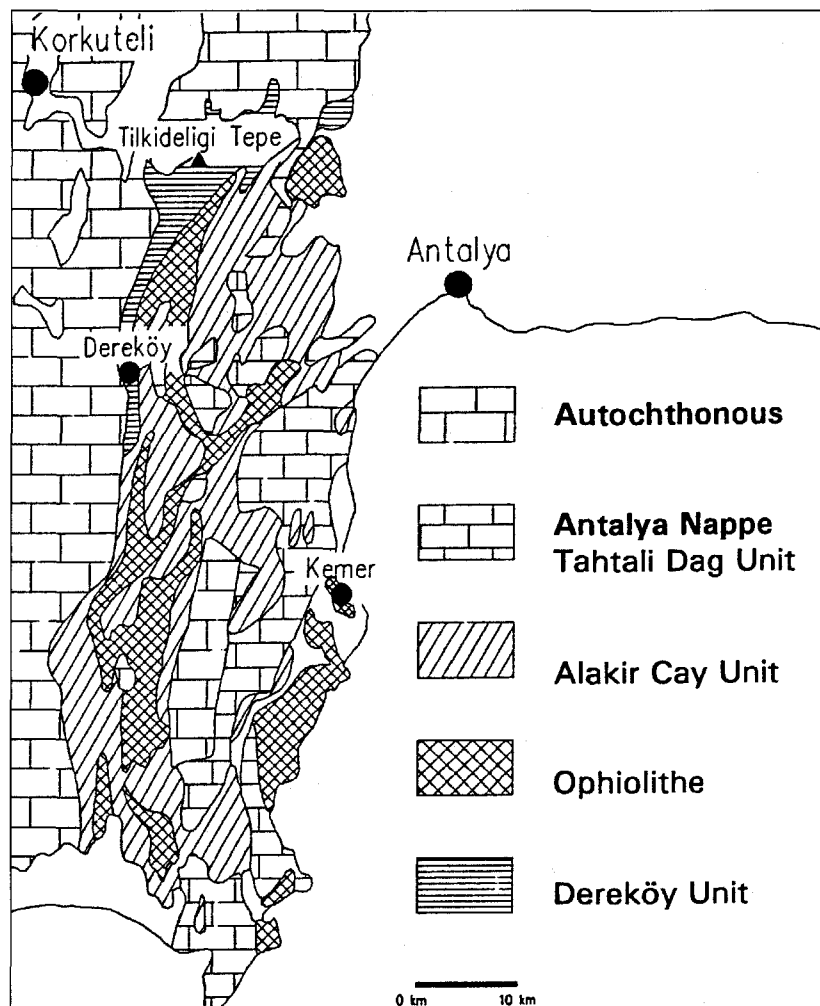
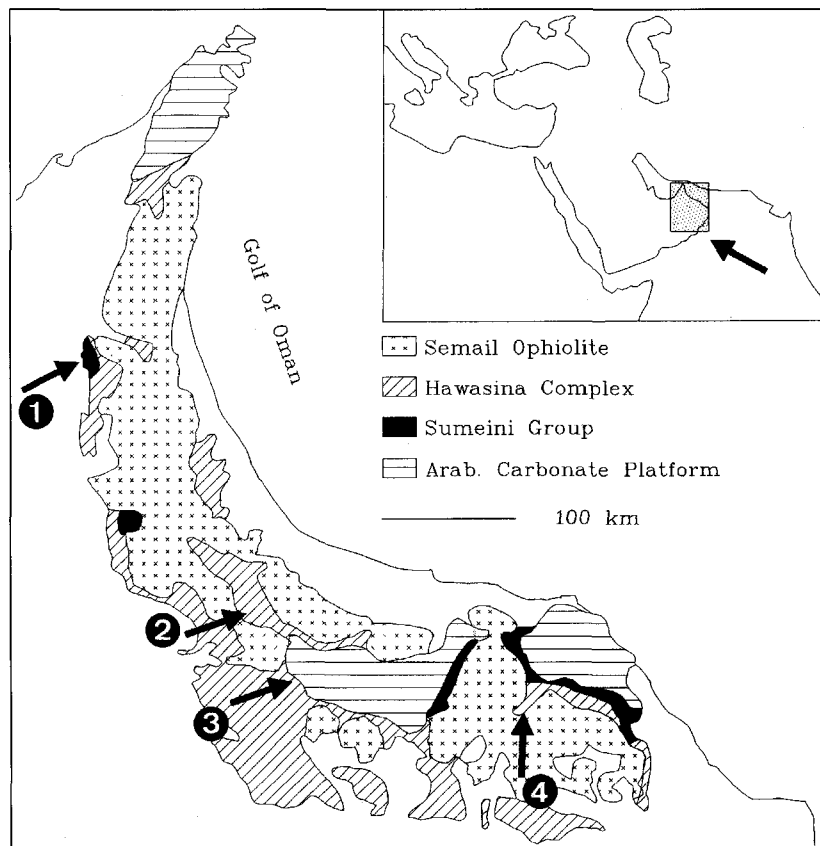
□ **Upper Permian reefal blocks of the Ba'id area, eastern Oman Mountains**
(Geological map of Fanjah; Explanatory notes by VILLEY et al. 1986)

Reefal blocks occur as isolated boulders or debris flows associated with other sediment gravity flow deposits, deep-water sediments and mafic volcanics. The sedimentary sequence was interpreted by BLENDINGER (1988) as a giant canyon infill from a former carbonate platform. Reefal blocks contain a rich fauna including "sphinctozoans", "inozoans", "chaetetids", rugose corals, hydrozoans, crinoids, bryozoans, *Tubiphytes*, and *Archaeolithoporella*. Aragonitic reefbuilders of the blocks are recrystallized in spite of their deposition as allochthonous blocks in a deeper marine setting.

□ **Upper Triassic reefbuilders of Jebel Kaur and Birkat al Mawz, central Oman Mountains**

A large Upper Triassic "Oman Exotic" from the Hawasina Nappes is in the Jebel Kaur. The limestones mainly represent sediments of a bedded shallow-water platform facies. In the northern part of the mountain (near the village of Sint), reefal limestones with dominant scleractinian corals and solenoporacean algae occur. The locality is not indicated as reefal limestone in the Geological Map of Rustaq (Geological map of Rustaq; Explanatory notes by BEURRIER et al., 1986).

In the area of Birkat al Mawz (Geological Map of Birkat al Mawz; Explanatory notes by HUTIN et al., 1986), reworked reefal blocks contain an Upper Triassic fauna of sponges, chaetetids, and corals. The aragonitic reefbuilders from all sites have been completely converted into calcite.



Text-Fig. 3.

Geological map east of Antalya, southern Turkey.

The samples were collected near Delictas/Dereköy in the Dereköy unit (after RIEDEL, 1990).

② Upper Triassic reefbuilders of the Sumeini Group (Oman Mountains)

The parautochthonous Sumeini Group is regarded as the former slope of the Arabian Platform (WATTS & GARRISON, 1986). The Wasa Formation mainly consists of a fore-reef breccia of an Upper Triassic shelf edge reef during the Carnian and Norian. The reworked reefbuilders mainly comprise sponges: "sphinctozoans", "inozoans", "chaetetids", and hydrozoans. Aragonitic reefbuilders are recrystallized.

③ Upper Triassic reefbuilders of western Taurus (Turkey)

The so-called Cipit-boulders of Norian age are well-known for their good preservation. The reefal blocks contain reefbuilders with unaltered aragonitic skeletons (CUIF, 1972). Common reefbuilders are scleractinians, "sphinctozoans", "inozoans", "chaetetids", spongiomorphids, and other "hydrozoans". Field data from the collected blocks were summarized by RIEDEL 1990 (sample localities near Delictas, Dereköy).

4. Data of Upper Permian and Upper Triassic Reefbuilders

For the following investigations "sphinctozoans", "chaetetids", and "hydrozoans" were used despite the polyphyletic origin of these groups (SENOWBARI-DARYAN, 1990; REITNER, 1992).

Quantitative data of the skeletonization are linked with taxonomy, description of gross morphology and microfacies analysis to provide a broad basis for discussion. Ske-

letonization was determined from both complete specimens and fragments. This chapter summarizes the important thin-section data for the discussion of the skeletonization. These data comprise growth morphology, dimension of skeletal elements and the quantitative data shown in Tabs. 1–6. Measured parameters of skeletal elements were listed in detail in order to try to document the variation within a colony level of different morphotypes as well as species.

4.1. "Sphinctozoans"

A selection of "sphinctozoans" from the study areas was analyzed. The most important genera for each study area were investigated, including common morphotypes of Upper Permian and Upper Triassic reefs such as moniliforme, catenulate, and glomerate growth forms. Thalamid sponges with filling structures or abundant vesiculae were also studied. Close-up views of the walls were only measured if they were pierced by coarse or labyrinthic pores. The taxonomy and terminology of the "sphinctozoans" are mainly based on SENOWBARI-DARYAN (1990, 1991).

4.1.1. Upper Permian "Sphinctozoans"

Of the 14 genera and 25 species of the Ba'id area 9 species were chosen here for measurement (Tab. 1).

Sollasia ostiolata STEINMANN, 1882

(Pl. 1/8, 11)

Gross morphology and skeletal elements: *S. ostiolata* is a small-sized sponge with a moniliform or multi-

Table 1.

Measured parameter of Upper Permian and Upper Triassic sphinctozoans.

Abbreviations in all tables: ° = unaltered reefbuilders; * = pores of the walls were measured separately and subtracted from the skeletonization; skel. [%] = skeletonization in area percent, skel. [g/cm³] = skeletal mass, long. = longitudinal section, obl. = oblique section.

taxon	sample	skel. [%]	mineralogy	skel. [g/cm ³]	section	age
<i>Thaumastocoelia?</i> sp.	SX	54	aragonite	1.57	long.	Upper Permian
<i>Thaumastocoelia?</i> sp.	SX	25	aragonite	0.74	long.	Upper Permian
<i>Sollasia ostiolata</i>	J1	35	aragonite	1.01	long.	Upper Permian
<i>Sollasia ostiolata</i>	ZT 54	45	aragonite	1.31	cross	Upper Permian
<i>Girtyocoelia beedi</i>	J2	32	aragonite	0.93	cross	Upper Permian
<i>Amblysiphonella merlai</i>	J1	24*	aragonite	0.7	long.	Upper Permian
<i>Amblysiphonella bancaensis</i>	ZT 8	24*	aragonite	0.7	cross	Upper Permian
<i>Amblysiphonella bancaensis</i>	ZT 8	25*	aragonite	0.73	cross	Upper Permian
<i>Parauvanella minima</i>	ZT 4	21	aragonite	0.61	oblique	Upper Permian
<i>Amblysiphonella? bullifera</i>	ZT 6	40*	aragonite	1.16	long.	Upper Permian
<i>Rhabdactinia columnaria</i>	ST	42	aragonite	1.22	cross	Upper Permian
<i>Salzburgia?</i> sp.	ZT 6	31	aragonite	0.89	cross	Upper Permian
<i>Uvanella? lamellata</i>	H9	50	Mg-calcite	1.35	cross	Upper Triassic
<i>Uvanella irregularis</i>	L19b	35	Mg-calcite	0.94	long.	Upper Triassic
<i>Alpinothalamia slovenica</i>	HS7b	33	Mg-calcite	0.89	long.	Upper Triassic
<i>Alpinothalamia bavarica</i>	LeK1	29	Mg-calcite	0.78	long.	Upper Triassic
<i>Alpinothalamia bavarica</i>	HS6	51	Mg-calcite	1.38	long.	Upper Triassic
<i>Alpinothalamia bavarica</i>	HS6	49	Mg-calcite	1.32	long.	Upper Triassic
<i>Alpinothalamia bavarica</i> °	19F1/3	36	Mg-calcite	0.97	cross	Upper Triassic
<i>Solenolmia manon manon</i>	H9	45	aragonite	1.31	long.	Upper Triassic
<i>Solenolmia manon manon</i>	H14	45	aragonite	1.31	long.	Upper Triassic
<i>Cryptocoelia zitteli</i>	H14	56	aragonite	1.62	long.	Upper Triassic
<i>Cryptocoelia zitteli</i>	H9	42	aragonite	1.22	cross	Upper Triassic

chambered growth form composed of bubble-like chambers. The species exhibit great variation with respect to gross morphology, chamber width and height as well as wall thickness.

Data: Calculation is derived from a longitudinal and a cross section. Cross section: chamber width 3.5 mm, thickness of wall 0.7 mm; longitudinal section: chamber width 3.1 mm, chamber height 3.2 mm, wall thickness 0.5 mm.

Preservation: The spherulitic microstructure can be observed in sample ZT 54 as relics indicating the good preservation of the skeleton in spite of recrystallization (Pl. 1/8).

***Thaumastocoelia?* sp.**

(Pl. 1/4, 7, 9, 10)

Gross morphology and skeletal elements: This species is composed of crescent-shaped chambers with a moniliform arrangement. Interwalls are truncated by pores; exowalls bear ostia. A considerable variation of wall thickness and chamber dimension is immediately obvious (see Pl. 1/4, 9).

Data: Calculation is based on drawings of two longitudinal sections. SX-1: chamber width 0.8–1.5 mm, thickness of wall 0.5–1.0 mm; SX-2: chamber width 1.5–2 mm, thickness of wall 0.3 mm.

Preservation: The skeletons are slightly silicified. Specimens are intergrown by other reefbuilders. Varying wall thickness is believed to be a primary feature, as indicated by external and internal biogenic incrustations and pores totally truncating the inner walls.

***Amblysiphonella bancaoensis* ZHANG, 1983;**

***Amblysiphonella merlai* PARONA, 1933**

Gross morphology and skeletal elements: These sponges are catenulate (ring-like chambers surrounding an axial spongocoel). The walls are pierced by numerous pores. Chambers and spongocoel may be filled by vesiculae. *A. bancaoensis* is a medium- to large-sized species and *A. merlai* is a medium-sized representative.

Data: A cross section (*A. bancaoensis*) and a longitudinal section (*A. merlai*) were analyzed from drawings. Cross section: total diameter 21 mm, chamber width 5 mm, spongocoel 11 mm, thickness of walls 1.1–2 mm. Longitudinal section: total diameter 9.2 mm, chamber width 3.1 mm, spongocoel 3 mm, thickness of wall 0.9–1 mm.

Preservation: Intrapores of both specimens are partly filled with sediment. Grey values of the recrystallized skeletons as well as different cements exhibit similar grey values. Micrite envelopes lined the walls and allowed cement and skeleton to be differentiated.

***Girtyocoelia beedei* (GIRTY), 1908**

Gross morphology and skeletal elements: Medium-sized *Girtyocoelia* of similar catenulate growth form, such as *Amblysiphonella* STEINMANN. Exowalls are pierced only by ostia and lack pores.

Data: A drawing of a cross section was analyzed: total diameter 5.7 mm, chamber width 1.8 mm, spongocoel 2.1 mm, thickness of wall 0.4 mm.

Preservation: Intraparticle pores are cemented and geopetally filled only by sediment. Micrite envelopes indicate the thickness of walls.

***Parauvanella minima* SENOWBARI-DARYAN, 1990**

Gross morphology and skeletal elements: The small-sized uniform sponge occurs as an encruster on and between larger reefbuilders. *Parauvanella* is composed of irregularly arranged chambers which exhibit great variation with respect to chamber size and wall thickness.

Data: A drawing was quantified. Chamber height and width varies between 0.5 and 1.6 mm, thickness of walls is 0.02 to 0.04 mm.

Preservation: The internal sediment of the chambers is partly recrystallized, with grey values very similar to those of the sponge skeleton. Chamber walls are lined by biogenic crusts or micrite envelopes.

***Salzburgia?* sp.**

Gross morphology and skeletal elements: Medium- to large-sized sponge which is composed of bubble-like chambers forming irregular aggregates. A central tube may be developed. The labyrinthic pore-network of the exowall is most characteristic (Pl. 1/6).

Data: Derived from drawings of a chamber. Chamber width 19 mm, thickness of wall 1 mm.

Preservation: The thickness of the partly micritic chamber walls can be recognized in the thin-section because of external encrustation by *Archaeolithoporella*. The intraparticle porosity is sealed by an interplay of multi-stage sedimentation and cementation. Early diagenetic radial fibrous cement can be distinguished from the wall lining.

***Amblysiphonella? bullifera* SENOWBARI-DARYAN & RIGBY 1988**

(Pl. 1/1–3, 5)

Gross morphology and skeletal elements: Medium-sized sponge with catenulate growth form.

Data: *A.? bullifera* was analyzed in a longitudinal section. A detail of the wall was also measured. The data are based on drawings: total diameter 17.5 mm, chamber width 5 mm, chamber height 8–11 mm, spongocoel diameter 7.5 mm, thickness of wall 1.5 mm.

Preservation: The specimen is encrusted by *Archaeolithoporella*, bryozoans, and chaetetics and incorporated in a framestone fabric. Micrite envelopes and internal sediment preserved details such as wall thickness and pores, despite the recrystallization of the skeleton and the cementation of the remaining pore space.

***Rhabdactinia columnaria* YABE & SUGIYAMA, 1934**

Gross morphology and skeletal elements: The large "sphinctozoan" is composed of crescentric

chambers pierced by well-defined tubes and pores. Tubes run through several chambers.

Data: A segment of a cross section was drawn for data evaluation. Chamber width 26 mm, thickness of tubes 2–3 mm, thickness of wall 2 mm.

Preservation: The specimen is badly preserved, owing to a lack of internal sediment, recrystallization, dolomitization and neomorphism of quartz. However, wall thickness is indicated by micritization. Pores in the wall cannot be quantified.

4.1.2. Upper Triassic "Sphinctozoans"

(Tab. 1)

***Alpinothalamia bavarica* (OTT), 1967;**

Alpinothalamia slovenica

(SENOWBARI-DARYAN) 1982

(Pl. 2/1, 2, 4, 6, 7, 9)

Gross morphology and skeletal elements: The cylindrical stems are characterized by a polyglomerate growth form (two or more layers of chambers surround an axial spongocoel). Chambers do not contain any filling structures but commonly bear vesiculae.

Data: Investigations were carried out on a specimen from Turkey (sample 19 F 1/3) and three specimens from the Oman Mountains (segments of longitudinal sections). Lek1 (Oman): total diameter 6 and 10 mm, width of chambers 2–4 mm, thickness of wall 0.1–0.3 mm; HS7b: total diameter 6 mm, width of chambers 0.3–1 mm, chamber height 0.3–0.7 mm, thickness of wall 0.1–0.2 mm; HS6: total diameter 10 mm, width of chambers 0.5–2 mm, chamber height 0.8–1 mm, thickness of wall 0.2–0.3 mm; 19F1/3 (Turkey): total diameter 7.5 mm, width of chambers 1.5 mm, thickness of wall 0.4 mm.

Preservation: The skeleton of *Alpinothalamia* is composed of recrystallization-resistant Mg-calcite. The specimens from both Turkey and Oman are therefore well-preserved and exhibit a distinct contrast to the surrounding cements.

***Solenolmia manon manon* (MÜNSTER), 1841**

Gross morphology and skeletal elements: *Solenolmia* commonly develops cylindrical stems with distinct segmentation. The chambers bear a reticulate filling structure. A retrosiphonate spongocoel is developed.

Data: Skeletonization was calculated from 2 longitudinal sections and a cross section. Longitudinal section: segment width 5–6 mm, segment height 3.5–4.5 mm, thick-

ness of fibres 0.2 mm, thickness of wall 0.2–0.3 mm; cross section H9a: segment width 3 mm, thickness of fibres 0.1 mm, thickness of wall 0.2 mm; longitudinal section H14: segment width 4.5 mm, segment height 2.5–3 mm, thickness of fibres 0.2 mm, thickness of wall 0.2 mm.

Preservation: The recrystallized skeleton is composed of a microgranular calcite differing from the surrounding cement with respect to crystal size and color. As a result of their different diagenetic histories, the cement and the recrystallized skeleton are characterized by different grey values, allowing measurement to be made without drawing.

***Uvanella? lamellata* SENOWBARI-DARYAN, 1981;**

***Uvanella irregularis* OTT, 1967**

(Pl. 2/3, 5, 8, 10)

Gross morphology and skeletal elements: This sponge is a multichambered aggregate composed of coarsely perforated chambers. Vesiculae may occur. *Uvanella* exhibits great variation with respect to growth form, total size, chamber size and the thickness of the walls.

Data: *U. lamellata*: Diameter of aggregate 5 mm, chamber width 0.7–1.5 mm, chamber height 0.2 mm, thickness of wall 0.1–0.5 mm. *U. irregularis*: Diameter of aggregate 8 mm, chamber width 3–4 mm, chamber height 0.8–1.2 mm, thickness of wall 0.1–0.2 mm.

Preservation: see *Solenolmia manon manon*.

***Cryptocoelia zitteli* STEINMANN, 1882**

Gross morphology and skeletal elements: *Cryptocoelia* is characterized by layered asiphonate or retrosiphonate chambers. Chambers are filled with a trabecular filling structure. Chambers may also bear vesiculae.

Data: Analysis was carried out on a longitudinal section (sample H14) and a cross section (H9). H14: Segment width 10 mm, chamber height 0.7–1.2 mm, thickness of fibres 0.1–0.2 mm, thickness of wall 0.1–0.2 mm; H9: Segment width 4.5 mm, thickness of fibres 0.1–0.2 mm, thickness of wall 0.1–0.2 mm.

Preservation: see *Solenolmia manon manon*.

4.2. Inozoans

(Tab. 2)

Inozoans have been poorly studied in comparison to "sphinctozoans". Determination at the genus or species

Table 2.
Skeletonization and skeletal mass of Upper Permian and Upper Triassic inozoans.

taxon	sample	skel. [%]	mineralogy	skel. [g/cm ³]	section	age
<i>Peronidella</i> sp.	ZT 54	55	aragonite	1.59	cross	Upper Permian
Genus et species indet. 1a	ZT 13	27	aragonite	0.78	long.	Upper Permian
Genus et species indet. 2	ZT 6-3	31	aragonite	0.89	oblique	Upper Permian
Genus et species indet. 1b	B4c	37	aragonite	1.07	cross	Upper Triassic
Genus et species indet. 1b	B4c	29	aragonite	0.84	cross	Upper Triassic
Genus et species indet. 2	Wa7	45	aragonite	1.31	oblique	Upper Triassic

level remains a matter of debate. Therefore, many inozoans are described here by an open nomenclature. Criteria for both Triassic and Permian inozoans are the presence/absence of spongocoel, the presence/absence of inhalent or exhalent canals, the consistency of the skeletal framework and the development of epitheca (DIECI et al., 1968; BIZZARINI & RUSSO, 1986; RIGBY et al., 1989).

4.2.1. Upper Permian Inozoans

Peronidella sp.

Gross morphology and skeletal elements: *Peronidella* HINDE 1893 develops a cylindrical growth form with a central tube. The sponge wall exhibits a reticular filling structure. The epitheca is constructed by a fusion of the fibres.

Data: A cross section was measured utilizing a drawing. Stem diameter 1.8 mm, central tube 0.5 mm, thickness of fibres 0.05 mm.

Preservation: The intraskeletal pores are cemented. The recrystallized skeleton is bordered by micrite envelopes.

Inozoan gen. et sp. indet. 1a

Gross morphology and skeletal elements: Cylindrical stems as well as incrusting aggregates. Exhalant canals and a spongocoel are missing. The sponge skeleton has a reticular structure.

Data: A close-up view was analyzed. Total sponge diameter 15 mm, thickness of skeletal fibres 0.2 mm, thickness of pores 0.2–1 mm.

Preservation: Intraparticle pores are filled with sediment, providing a contrast to the recrystallized skeleton.

Inozoan gen. et sp. indet. 2

Gross morphology and skeletal elements: This inozoan consists of cylindrical stems with a central tube and inhalent/exhalent channels. A reticulate skeleton is developed. Walls are constructed by a fusion of the skeleton.

Data: A cross section comprising central tube, inhalent/exhalent tubes, reticulate skeleton and cortex were studied. Total diameter 10 mm, spongocoel 1.9 mm, thickness of inhalent/exhalent channels 0.7–1 mm, thickness of pores 0.4–0.8 mm, thickness of skeletal fibres 0.05–0.2 mm.

Preservation: The sponge is incorporated into a biogenic framework by incrustations of *Archaeolithoporella*, *Tubiphytes*, and chaetetids. Intraskeletal pores are filled with sediment, in contrast to the recrystallized skeleton.

4.2.2. Upper Triassic Inozoans

Inozoan gen. et sp. indet. 1b

Gross morphology and skeletal elements: This inozoan is similar in the arrangement of its skeletal elements to inozoan sp. et gen. indet. 1a.

Data: An overview and a close-up view were investigated. Total diameter 15 mm, thickness of skeletal fibres 0.3–0.4 mm.

Preservation: Intraskeletal pores were cemented by radial fibrous calcite prior to dissolution of the aragonitic sponge skeleton. As a result of a late diagenetic overprint, the marine phreatic cement has a dull appearance in contrast to the bright sparry calcite of the recrystallized skeleton.

Inozoan gen. et sp. indet. 3

(Pl. 3/1–3)

Gross morphology and skeletal elements: The inozoan has a cylindrical growth form. It is characterized by dichotomously branching canals. The sponge has a reticular skeleton. A close-up view including canals and skeletal fibres were analyzed.

Data: Total diameter 9.5 mm, thickness of tubes 0.7–0.9, thickness of fibres 0.1–0.3 mm.

Preservation: The intraskeletal pores were filled with sediment prior to recrystallization of the aragonitic skeleton, thus emphasizing the primary skeletal mass.

4.3. Chaetetids and Hydrozoans

Owing to great differences in the taxonomy, only a general description at genus level is given. As a result of the complex arrangement of the skeletal elements, data evaluation is better carried out directly from thin-sections than from drawings.

4.3.1. Upper Permian Chaetetids

(Tab. 3)

Chaetetetes sp.

(Pl. 4/4, 5, 7)

Gross morphology and skeletal elements: Chaetetids exhibit great variability with respect to growth form occurring as domical colonies, tabular colonies or incrusters on other reefbuilders (WEST & KERSHAW, 1991). The skeleton is hemispherical and composed of very slender tightly packed tubes.

Data: Sample SL: diameter of colony 1.2 mm, tube diameter 0.3 mm, wall diameter 0.1 mm (cross section).

Preservation: The originally aragonitic skeleton is recrystallized.

Table 3.
Skeletonization and skeletal mass of Upper Permian and Upper Triassic chaetetids.

taxon	sample	skel. [%]	mineralogy	skel. [g/cm ³]	section	age
<i>Chaetetetes</i> sp.	SL	46	aragonite	1.34	cross	Upper Permian
<i>Bauneia</i> sp.	B4a	56	aragonite	1.62	cross	Upper Triassic
<i>Bauneia</i> sp.	B6a	58	aragonite	1.69	long.	Upper Triassic
<i>Atrochaetetetes medius</i> ^o	19F33	52	aragonite	1.51	long.	Upper Triassic

4.3.2. Upper Triassic Chaetetids

(Tab. 3)

Systematic investigations of post-paleozoic chaetetids were done by FISCHER (1970). The well-preserved material of Turkey was studied by CREMER (1993) in his diploma thesis.

Atrochaetetes medius CUIF & FISCHER, 1974

(Pl. 4/6)

Gross morphology and skeletal elements: The colonies have a globular to bell-shaped growth form. Tubes with distinct walls are round to oval in cross section. Walls are aperforate and exhibit narrow bands of slower growth.

Data: Sample 19F33: Tube diameter 0.7–0.3 mm, wall diameter 0.1–0.2 mm (longitudinal section).

Preservation: The aragonitic skeleton is well preserved.

Bauneia sp.

Gross morphology and skeletal elements: The colony is large and exhibits indistinct growth elements. Slender tubes with thick walls and scarce tabulae produce a rounded internal section.

Data: Sample B4a: Diameter of colony 3.3 mm, tube diameter 0.6–0.7 mm, wall thickness 0.1–0.2 mm (cross section); sample B6a: Tube diameter 0.6–0.7 mm, wall thickness 0.1–0.2 mm (longitudinal section).

Preservation: The skeletons are recrystallized. The tightly packed skeletal elements with numerous vertical tabulae prevent an infill of sediment in the intraskeletal space.

4.3.3. Problematical Upper Permian Hydrozoans

(Tab. 4)

FAN et al. (1991) described abundant reefbuilders from Middle and Upper Permian reefs as 'hydrozoans'. These organisms may be representatives of the inozoans (SENOWBARI-DARYAN, pers. communication). The term is therefore used with caution.

Pseudopalaeoaplysina sp.

(Pl. 4/8,9)

Gross morphology and skeletal elements: This species commonly develops slender stems. In cross

section, tubes radiate from the center to the margin of the colony exhibiting an indistinct trabecular structure. In oblique sections however, only an irregular skeleton is visible.

Data: A longitudinal section was analyzed from a drawing: stem diameter 7–10 mm, thickness of skeletal fibres 0.05–0.2 mm, size of intraskeletal pores 0.2–0.7 mm.

Preservation: Recrystallization of the internal sediment partly reduced the contrast to the recrystallized skeleton. Therefore, a drawing was studied.

Radiotrabeculopora sp.

Gross morphology and skeletal elements: Colonies are commonly of globular growth form. A distinct trabecular structure can be observed in longitudinal section. Single tubes run parallel to the longitudinal axis or may radiate slightly to the margin.

Data: A longitudinal section was analyzed. Thickness of skeletal fibres 0.1–1 mm, size of pores 0.1–1 mm.

Preservation: Intraskeletal pores are filled with sediment and provided enough contrast for direct data evaluation.

4.3.4. Upper Triassic Hydrozoans

(Tab. 4)

The general term "hydrozoans" is often used because of systematic discussions. Abundant reef builders in the Upper Triassic of Oman are spongiomorphids and disjectopora.

Spongiomorpha ramosa FRECH, 1890

(Pl. 3/7–9)

Gross morphology and skeletal elements: The shape and size of the entire colony is unknown; only broken branches are preserved. Massive vertical elements dominate, united by annular thickenings or by horizontal bars.

Data: Thin-section Wa2b: Thickness of branches 1 cm; thickness of vertical elements 0.15–0.25 mm; horizontal elements 0.05–0.15 mm.

Preservation: The branches are recrystallized and very slightly dissolved.

Disjectopora sp.

(Pl. 3/4–6)

Gross morphology and skeletal elements: Knobby or mushroom shape massive colonies show re-

Table 4.
Skeletonization and skeletal mass of Upper Permian and Upper Triassic hydrozoans.

taxon	sample	skel. [%]	mineralogy	skel. [g/cm ³]	section	age
<i>Pseudopalaeoaplysina</i> sp.	ZT 13	48	aragonite	1.39	long./obl.	Upper Permian
<i>Radiotrabeculopora</i> sp.	SC	54	aragonite	1.57	long.	Upper Permian
<i>Disjectopora</i> sp.	I30a	42	aragonite	1.22	cross.	Upper Triassic
<i>Disjectopora</i> sp.	I30a	39	aragonite	1.13	cross/obl.	Upper Triassic
<i>Spongiomorpha ramosa</i>	Wa2bs	49	aragonite	1.42	long.	Upper Triassic
<i>Spongiomorpha ramosa</i>	Wa2bs	47	aragonite	1.36	long.	Upper Triassic

Table 5.
Skeletonization and skeletal mass of Upper Permian ceroid Rugosa.

taxon	sample	skel. [%]	mineralogy	skel. [g/cm ³]	section	skeletal elements
<i>Wentzelella W. annae</i> ^o	ZT 21	47	Mg-calcite	1.27	long.	dissepiments
<i>Wentzelella W. annae</i> ^o	ZT 44	43	Mg-calcite	1.16	long.	dissepiments
<i>Wentzelella W. annae</i> ^o	ZT 33	50	Mg-calcite	1.35	cross	columella, septa
<i>Wentzelella W. annae</i> ^o	ZT 33	58	Mg-calcite	1.57	cross	septa, wall
<i>Wentzelella W. annae</i> ^o	ZT 38	49	Mg-calcite	1.32	cross	calices
<i>Wentzelella W. annae</i> ^o	ZT 38	50	Mg-calcite	1.31	cross	columella, septa
<i>Wentzelella W. annae</i> ^o	ZT 38	51	Mg-calcite	1.38	cross	septa, wall
<i>Wentzelella W. wynnei</i> ^o	ZT 43	61	Mg-calcite	1.65	cross	columella, septa
<i>Wentzelella W. wynnei</i> ^o	ZT 43	54	Mg-calcite	1.46	cross	wall, septa

gular trabecular skeleton traversed by strong continuous vertical astrorhizae.

Data: Two close-up views were analysed. Thin-section 130a: Size of colony 1.4 cm; thickness of trabeculae 0.05–0.15 mm; diameter of astrorhizae 0.5–0.6 mm.

Preservation: Intratrabecular cavities and vertical astrorhizae are filled with sediment, providing enough contrast for measurement.

Hydrozoa gen. et. sp. indet.

(Pl. 4/1–3)

Gross morphology and skeletal elements: The coenosteum is trabecular in structure. Stellate patterns of laterally extended branches of canals are visible. Growth banding is weakly developed.

Data: Thin-section 19A1/2: Size of colony 7 cm, thickness of trabeculae 0.05–0.1 mm, extension of canals 2–4 mm.

Preservation: The specimen of the Cipit Boulders of Turkey is well preserved. The dark skeleton provides a distinct contrast to the absolutely clear intrapore cement.

4.4. Upper Permian Rugose Corals

(Tab. 5, Pl. 5)

Rugose corals are represented in the Oman Mountains by cerioid, dendroid, and solitary growth forms. Cerioid morphotypes are most abundant and were described by BLENDINGER & FLÜGEL (1990). Only cerioid forms were studied in this paper.

Wentzelella (Wentzelella) wynnei

(WAAGEN & WENTZEL) 1886;

Wentzella (Wentzella) annae

BLENDINGER & H.W. FLÜGEL, 1990

Gross morphology and skeletal elements: The cerioid colonies exhibit a subglobular shape. In cross section the corallites are polygonal (commonly 5–6 sides) and vary in size. Columella, tabulae and dissepiments are developed. The walls are constructed by fusion of the septa, forming a zigzag line. In longitudinal section distinct growth banding may be developed.

Data: Measurements comprise overviews and close-up views of longitudinal and cross sections. Cross sections: ZT 33: diameter of eroded corallite fragment 9 x 15 mm, columella 2.5 x 1.2 mm, thickness of septa 0.05–0.2 mm, thickness of wall 0.3–0.8 mm; ZT 38: size of corallum not known because of erosion, diameter of corallite 12 x 18 mm, diameter of columella 3 x 2.1 mm, thickness of septa 0.05–0.2 mm, thickness of wall 0.3–1 mm; ZT 43: eroded corallite diameter 10 x 8 mm, diameter of columella 1.8 mm, thickness of septa 0.5–1.5 mm, thickness of wall 1 mm. Longitudinal sections: ZT 21, thickness of dissepiments 0.1 mm, ZT 44, thickness of dissepiments 0.05–0.1 mm.

Preservation: All specimens are well preserved as a result of the stable Mg-calcitic skeletal mineralogy. Measurements were carried out directly. Some calices are silicified, enhancing the contrast to the intraskeletal pores.

4.5. Upper Triassic Scleractinians

(Tab. 6)

Owing to their aragonitic origin triassic scleractinians are often badly preserved or completely dissolved. There-

Table 6.
Skeletonization and skeletal mass of Upper Triassic scleractinians.

taxon	sample	skel. [%]	mineralogy	skel. [g/cm ³]	morpholog	section	skeletal elements
<i>Seriastrea multiphylla</i>	KX 4-1	50	aragonite	1.45	cerioid	long.	septa, dissepiments
<i>Isastraea sp.</i> ^o	19A2	53	aragonite	1.53	cerioid	cross	calices
<i>Isastraea sp.</i> ^o	19A2	52	aragonite	1.51	cerioid	cross	calices
<i>Retiophyllia sp.</i>	DK 3	36	aragonite	1.04	dendroid	cross	septa, dissepiments
<i>Retiophyllia sp.</i>	LE 1	28	aragonite	0.81	dendroid	cross	septa
<i>Montlivaltia sp.</i>	JS1	31	aragonite	0.9	solitary	cross	septa, wall
<i>Montlivaltia sp.</i> ^o	19A11	34	aragonite	0.99	solitary	cross	septa, columella

fore, the data base comprises only a few measurements. Most of the material comes from the Cipit boulders of Turkey which still yield aragonitic reefbuilders.

Seriastrea multiphylla
SENOWBARI-DARYAN & SCHÄFER, 1978
 (Pl. 6/8, 11, 12)

Gross morphology and skeletal elements: Laminar and massive corallum with numerous small coral-lites.

Data: A longitudinal section was investigated. Height 5 mm, thickness of septa 0.1–0.2 mm, interseptal space 0.2 mm.

Preservation: Interseptal space was filled with micrite prior to recrystallization of the skeleton. The colony is partly bored and colonized by *Spongiostromata*-crusts and *Microtubus communis* FLÜGEL.

***Isastrea* sp.**
 (Pl. 6/7, 9, 10)

Gross morphology and skeletal elements: Massive corallum composed of cerioid corallites. About 30 septa are arranged in three orders. A distinct axial structure is absent.

Data: The corallites were analyzed in cross sections (detail and overview). The original size of the colony is unknown owing to erosion. Diameter of corallite 5–7 mm, thickness of wall 0.3–0.4 mm, thickness of septa 0.14–0.2, interseptal space 0.3–0.4 mm.

Preservation: The specimens of the Cipit Boulders are very well preserved.

***Retiophyllia*-Type**
Dendroid Scleractinian Colony

Gross morphology and skeletal elements: The corals exhibit a dendroid growth form with intratentacular budding. Each stem develops one calyx only. Calices are probably composed of at least two cycles of septa. Dissepiments are common. The wall is septothecal.

Data: Two close-up views of cross sections were measured. Thin-section DK 3: Calyx diameter 8 mm, thickness of septa 0.05–0.2 mm (depending on cycle of septa), thickness of dissepiments 0.0–0.03 mm, interseptal space 0.7–0.9 mm; thin-section Le 1: Calyx-

diameter 7–8 mm, thickness of septa 0.1 mm, interseptal space 0.02 mm.

Preservation: Interseptal space of the calices of thin-section DK 3 is filled with micrite. Cements of the interseptal space of thin-section Le 1 differ from the recrystallized septa with respect to color and size.

***Montlivaltia*-Type**
Solitary Scleractinian
 (Pl. 6/1–6)

Gross morphology and skeletal elements: Large conical calices with at least 3 cycles of septa. An axial structure (columella) is weakly developed.

Data: Two close-up views of cross sections were analyzed. Thin-section JS1: Coral diameter 30 mm, thickness of septa 0.2 mm, interseptal space 0.5 mm; thin-section 19A11: Coral diameter 40 mm, thickness of septa 0.2 mm, interseptal space 0.3–0.5 mm. Solitary corals with several septal cycles or a complex dissepimentarium are especially difficult to draw and are better measured directly from thin-sections.

Preservation: Both specimens exhibit a different preservation and are regarded as end members of comparable samples for quantification. Sample 19A11 from the Cipit Boulders of Turkey consists of the primary aragonite. The skeleton is dark as compared to the surrounding cement, thus exhibiting good contrasts. Sample JS1 of the Oman Mountains is a specimen with a typically recrystallized skeleton. Relic structures of the skeleton do not exhibit enough contrast to the surrounding cements; hence the skeletonization can be quantified only with difficulty.

5. Interpretation

5.1. Discussion of Data

The quantitative data comprise (a) the skeletonization of reefbuilders in area percent and (b) the skeletal mass calculated as the skeleton in g/cm³ (density of aragonite = 2.9 g/cm³, density calcite = 2.7 g/cm³). Both parameters were evaluated for individual reefbuilders (Tabs. 1–6) and higher taxa (Tab. 7). The skeletonization was transformed into skeletal mass in order to facilitate the comparison to data of modern reefbuilders.

Quantitative data on the skeletonization or skeletal mass of ancient reefbuilders are rare. The basic question

Table 7.
 Skeletonization and skeletal mass of higher taxonomic taxa.

Higher taxa	Skeletonization [%]	Mean skelet. [%]	Skeletal mass [g/cm ³]	Mean skel. mass [g/cm ³]	Number (N) of measurements
Sphinctozoans, Upp. Permian	21 - 54	33	0.7 - 1.57	0.96	12
Sphinctozoans, Upp. Triassic	29 - 56	43	0.78 - 1.62	1.19	11
Inozoans	27 - 55	37	0.78 - 1.59	1.08	6
Solitary scleractinians	31 - 34	33	0.9 - 0.99	0.95	2
Dendroid scleractinians	28 - 36	32	0.81 - 1.04	0.93	2
Cerioid scleractinians	50 - 53	52	1.45 - 1.53	1.5	3
Cerioid Rugosa	43 - 61	51	1.16 - 1.65	1.39	9
Chaetetids	46 - 58	53	1.34 - 1.69	1.54	4
Hydrozoans	39 - 54	47	1.13 - 1.57	1.3	6

is whether the data really reflect the primary skeleton or whether they infer misinterpretations, owing to the diagenetic overprint. However, the combination of quantitative analysis and microfacies studies provides the basis for a critical discussion. According to sedimentological and paleontological arguments, the data provide a good data base of the amount of the skeletal material, because

- well-preserved reefbuilders from the Cipit boulders do not differ significantly in the variability from their recrystallized counterparts,
- fine-grained sediments filling the intraskeletal pores were lithified prior to the recrystallization of the metastable skeleton and preserved the skeletal architecture (e.g., Pl. 3/1),
- biogenic incrustations indicate the dimensions of skeletal elements (e.g., Pl. 1/3),
- micrite envelopes and early marine cements rimmed their substrate and documented the skeletal architecture (e.g., Pl. 1/2),
- relic structures such as pores are restricted to the (recrystallized) skeleton and cannot be traced into surrounding cements (e.g., Pl. 1/9).

However, the number of successfully treated samples indicates differences with respect to the value of data in the discussion of the skeletonization (Tab. 7). Sphinctozoans, inozoans, cerioid rugose corals and hydrozoans are characterized by a higher number of measurements, whereas scleractinians and chaetetids were analyzed on the basis of only a few samples, owing to differences in mineralogy, arrangement of skeletal elements and preservation. Chaetetids and scleractinians, characterized by tightly packed skeletal elements which prevent the infill of sediment (Pl. 4/4–7), and metastable aragonitic skeletons are therefore poorly preserved in many cases. Reefbuilders which developed more loosely packed skeletal elements (e.g., sphinctozoans, Pls. 1/1,8) or secreted stable skeletons (low Mg-calcite, rugose corals) are characterized by better preservation. Therefore, data of recrystallized skeletons of sphinctozoans, inozoans and hydrozoans are regarded to be more reliable than those for scleractinians and chaetetids.

5.2. Discussion of the Reefbuilders

(Text-Figs. 4–5)

Sphinctozoans

The mean value of skeletonization (average of all measurements) varying from 33 to 43 % initially suggests a weak skeletonization, but individuals exhibit considerable variation ranging from 21–56 %. The reasons for the variation are:

- a) Different morphotypes comprising moniliform, catenulate, and polyglomerate arrangement of chambers as well as the presence or absence of a filling structure.
- b) Despite different morphotypes, sphinctozoans exhibit extreme variability with respect to chamber height, chamber width and wall thickness.

SENOWBARI-DARYAN (1990) emphasizes the variation of these parameters for different species of *Amblysiphonella* (SENOWBARI-DARYAN, 1990: Tab. 10), *Sollasia ostiolata* (SENOWBARI-DARYAN, 1990, p. 128), and *Alpinothalamia* (SENOWBARI-DARYAN, 1990: Fig. 49). Intraspecific variation is also obvious in the material studied for *Thaumastocoelia*, *Uvanella* and *Alpinothalamia* (see measured parameters of skeletal elements on pages 36 and 37). As a result of the intraspecific variation, a positive correlation of complex growth forms such as polyglomerate stems (e.g., *Alpinothalamia*) and skeletonization is not always recognizable. Thick-walled sphinctozoans of primitive chamber arrangement (e.g. moniliform arrangement of chambers, *Thaumastocoelia* sp.) may develop a similar rate of skeletonization as complex types.

Inozoans

Data for inozoans are comparable to those for sphinctozoans in regard to the extreme variability of skeletonization (27–55 %) with a mean of 37 %; this is surprising, because inozoans are characterized by different types of filling structure.

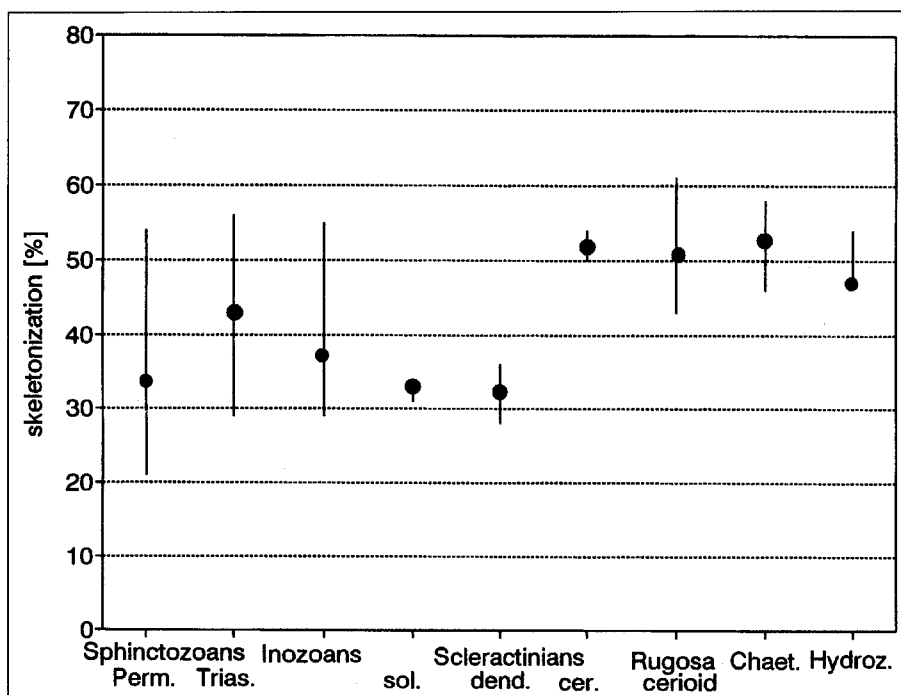
Solitary/dendroid/cerioid scleractinians

The skeletonization of recrystallized specimens of the Oman Mountains may be calculated too high due to diagenesis. The aragonitic scleractinians of Turkey exhibit distinct contrasts and provide useful data.

The following trends can be observed:

- a) solitary and dendroid scleractinians secreted relatively weak skeletons;
- b) cerioid scleractinians are well skeletonized;
- c) differences in the mean skeletal mass are considerable: Dendroid and solitary scleractinians consist of about 30 % skeleton and 50 % cerioid forms.

The ontogenetic development may have had great influence on the variation of skeletonization.



Text-Fig. 4.
Variation and mean skeletonization of higher taxa.

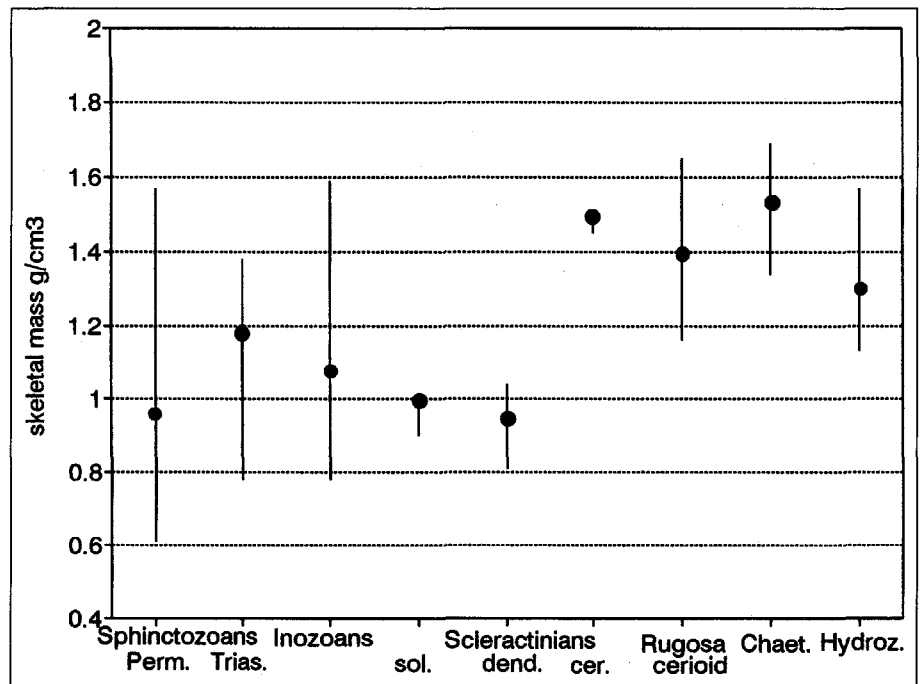
Text-Fig. 5.
Variation and mean of skeletal mass of
higher taxa.

Ceriod rugose corals

Despite their phylogenetic origin, the skeletonization of ceriod rugose corals is similar to ceriod scleractinians. Both variation (43–61 %) and mean (51 %) suggest a strong skeletonization.

Chaetetids and hydrozoans

Chaetetids and hydrozoans are comparable to other well skeletonized reefbuilders e.g. ceriod Rugosa and ceriod scleractinians with respect to variation of skeletonization (39–58 %) and mean skeletonization (53 %, 47 %).



5.3. Application of Quantitative Skeleton Data: Recognition of Reefbuilding Guild Attribution

According to FAGERSTROM (1987, 1991) reef organisms can be assigned to three guilds: constructor, baffler and binder. The attribution of the reef-building guilds is based on a hierarchical checklist given by FAGERSTROM (1991), see Tab. 8. Growth direction, gross morphology and skeletonization of reefbuilders are regarded as important criteria for guild assignment. The quantitative data evaluated in our study allow a refinement of the guild concept with regard to the definition of guild types. Different guilds are defined by differences in mean skeletonization and

mean skeletal mass. Two major groups are evident in our material (Figs. 4–5):

- 1) Well-skeletonized reefbuilders with a mean skeletonization of about 50 % can be assigned to the constructor guild. Common representatives are ceriod rugose corals, ceriod scleractinians, chaetetids and hydrozoans.
- 2) Weakly skeletonized reefbuilders with a mean skeletonization of 30–40 % contribute to the baffler guild and are represented by many sphinctozoans, inozoans, solitary scleractinians and dendroid scleractinians.

Table 8.

Hierarchical check list for the determination of reefbuilding guilds.

The skeletonization of reefbuilders is an important criterion for guild assessment (after FAGERSTROM, 1991).

	Criteria	Constructor	Baffler	Binder
1	habit growth habit growth direction	upwards erect	upwards erect	lateral reptant
2	life-form growth form form	massive, domes branches, cups columns	cylinders, cones blades	sheets, lenses runners, webs plates, umbrellas
3	skeletonization skeletal strength and rigidity	well-skeletonized strong, rigid	poorly skeletonized mostly as skeletal fragments	well-skeletonized
4	skeletal volume coloniality	large, colonial or gregarious	smaller, solitary or colonial	medium size colonial or gregarious
5	biostratonomy taphonomy transportability	in growth position or in situ (toppled, broken)	in situ (toppled; broken) commonly transported	in growth position encrust, roof-over or trap sediment
6	skeletal packing density	as in life or less dense	highly variable from disperse to concentrated	as in life

Variation, especially in the skeletonization of sphinctozoans and inozoans, indicates a considerable guild overlap from weakly skeletonized bafflers and well skeletonized constructors. The data, therefore, strongly support FAGERSTROM (1991), who requires guild assignment for individual reefbuilders rather than for higher taxonomic groups.

Guild assignment of sphinctozoans and inozoans must consider the wide range of morphotypes as well as variations in chamber height, chamber width and wall thickness.

5.4. Ancient Versus Modern Skeletal Density: An Attempted Comparison

Variations in the skeletal mass are a well-known phenomenon of modern reefbuilders and have been studied with statistical methods. FORSTER (1985) detected different levels of variation, including inter-colony variation, variations between colonies of a population and variations between different populations of the reef coral *Montastraea*. She explained these variations with a complex network of growth rate, calcification, reproduction and nutrition. Growth bands in massive corals comprising low density and high density couplets may document seasonal variations. In addition, BOSSCHER (1992) observed an increase in skeletal density of *Montastraea*, which increased with depth as a result of reduced growth rate.

The quantitative analysis of the Upper Permian and Upper Triassic reefbuilders indicates that this phenomenon can be traced in the geological rock record. The possible level of variation is difficult to recognize owing to a lack of data: Variations between reefbuilders belonging to the same species were observed from more detailed data sets of the sphinctozoans (e.g. *Thaumastocoelia?* sp. Pl. 1/4, 9 or *Alpinothalamia bavarica*, Pl.2/2,9; Tab. 1) and rugose corals (e.g. *Wenzelella W. annae*, Tab. 5). Rugose corals exhibit growth bands in longitudinal section, explaining differences in skeletonization (Tab. 5, Pl. 5/3). Mechanisms trig-

gering the variations cannot yet be concluded from our data set.

6. So, What Potential Does this Technique Have?

Primary data on skeletonization and skeletal mass may be influenced by a complex interplay of triggering mechanisms, like diagenesis, size of measured areas and kind of section. The combination of quantitative analysis and qualitative observations (microfacies analysis and carbonate petrography) enables skeletonization and skeletal mass of ancient reefbuilders to be realistically reconstructed. Primary signals such as differences in morphotypes, intraspecific variation and inter-colony variation affect skeletonization.

Quantitative skeleton data are important in the discussion of the rigidity of reef organisms over time (SCHUHMACHER & PLEWKA, 1981), changes in debris production of different architectural reef classes (GERHARD, 1991), changes in the carbonate net production in reefs (HUBBARD et al., 1990). Our study focuses on the differences in the intensity of skeletal growth and on the potential for using these differences in the recognition of reef guilds.

Acknowledgements

The authors thank the Ministry of Petroleum and Minerals of the Sultanate of Oman and Dr. Hilal AL-AZRI for their support in Oman. P. RIEDEL (Plauen) and B. SENOWBARI-DARYAN (Erlangen) provided us with material from Turkey (Delictas near Dereköy, southern Turkey) and H. CREMER (Erlangen) determined the chaetids. J.A. FAGERSTROM (Boulder, Colorado) and B. SENOWBARI-DARYAN (Erlangen) kindly reviewed the manuscript. M. NEUFERT did the microphotographs. The investigations were supported by the Deutsche Forschungsgemeinschaft (Project FI 42/62-1/2) within the Priority Project 'Global and Regional Controls on Biogenic Sedimentation'. O. WEIDLICH was funded by a grant of the Graduiertenförderung of the Friedrich-Alexander-Universität Erlangen-Nürnberg.

Plate 1

Microphotographs and laser prints of Upper Permian sphinctozoans.

The black areas of all laser prints represent the skeleton of the reefbuilders and are calculated with respect to skeletonization and skeletal mass. The combination of microphotographs and corresponding laser prints is believed to indicate whether data evaluation must be interpreted with caution. Reefbuilders with preserved original mineralogy are especially suitable for study.

- Fig. 1: ***Amblysiphonella? bullifera* SENOWBARI-DARYAN & RIGBY 1988.** Longitudinal section of a catenulate stem with spongocoel, ring-like chambers and filling structure. The aragonitic skeleton has turned into calcite. Sample ZT 6; $\times 2.5$.
- Fig. 2: **Detail of *Amblysiphonella? bullifera*.** The exowalls are pierced by pores. The original skeleton is recognizable despite recrystallization, owing to biogenic crusts (*Archaeolithoporella hidensis*), sediment infill and micrite envelopes. Sample ZT 6; $\times 16$.
- Fig. 3: **Close-up view of Fig. 1.** The exowall and filling structure of *Amblysiphonella? bullifera* exhibit the same thickness in the sediment-filled area as well as in the cemented area of the intraparticle pore as a result of early micritization. Sample ZT 6; $\times 12$.
- Fig. 4: ***Thaumastocoelia?* sp.** Longitudinal section of the moniliforme sponge composed of crescent-shaped chambers. Sample SX; $\times 4.5$.
- Fig. 5: **Laser print of the wall of *Amblysiphonella? bullifera* from a drawing.** The complex network of crystals prevented a direct measurement of the close-up view. Sample ZT 6; $\times 20$.

- Fig. 6: **The laser print of a drawing exhibits the labyrinthic character of the pores piercing the wall of *Salzburgia?* sp.** Sample ZT 6; $\times 17$.
- Fig. 7: **Laser print of *Thaumastocoelia?* sp. from Fig. 4.** The quantitative analysis is based on a drawing. Direct measurement from a microphotograph was impossible because of similar grey values from the recrystallized skeleton and cements of the intraparticle pore. Sample SX; $\times 6.5$.
- Fig. 8: ***Sollasia ostiolata* STEINMANN 1882.** The spherulitic microstructure is preserved in relics despite recrystallization. Sample ZT 54; $\times 14$.
- Fig. 9: ***Thaumastocoelia?* sp.** The walls are very thick in contrast to the specimen figured in Pl. 1/4. Sediment infill, biogenic incrustations and preserved pores indicate that the thickness of the walls also represents the original dimension of the skeletal elements. Sample SX; $\times 3.5$.
- Fig. 10: **Laser print of *Thaumastocoelia?* sp. from Fig. 9.** Sample SX; $\times 5.5$.
- Fig. 11: **Laser print of *Sollasia ostiolata* from Fig. 8.** Sample ZT 54; $\times 8.5$.

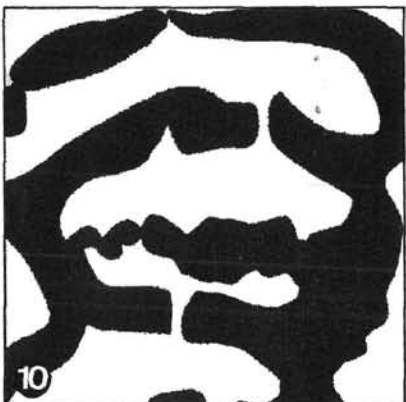
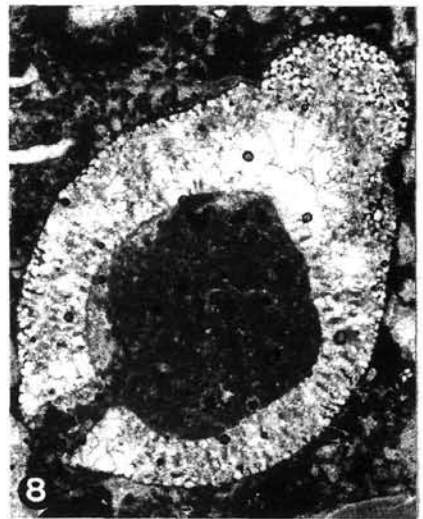
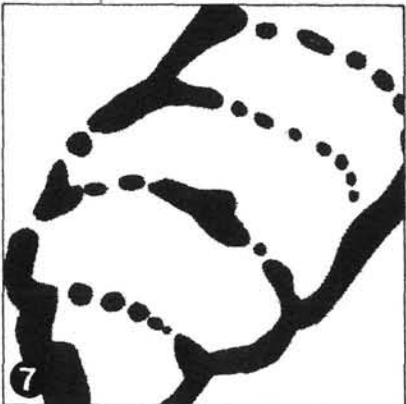
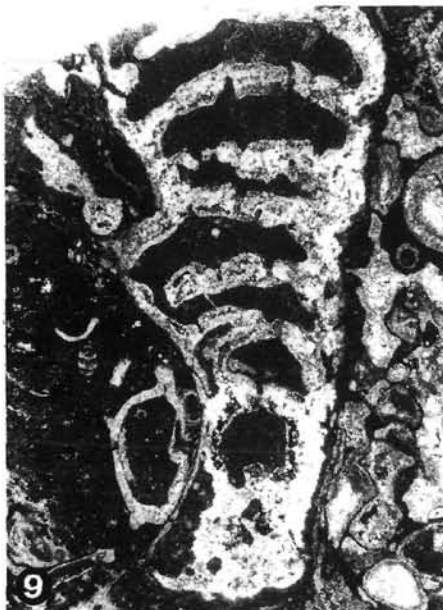
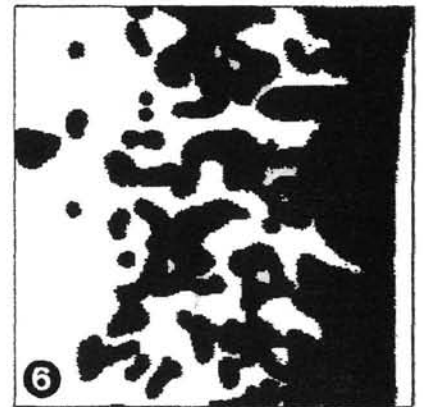
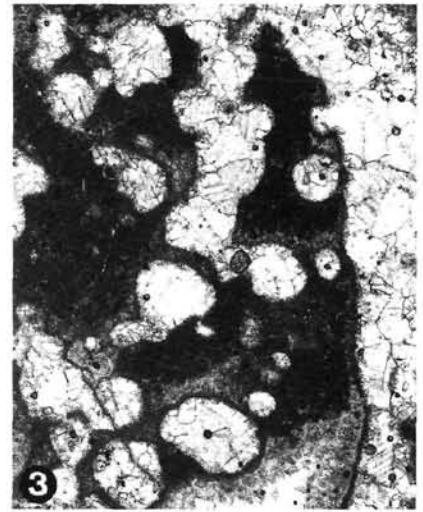


Plate 2

Microphotographs and laser prints of Upper Triassic sphinctozoans.

- Fig. 1: ***Alpinothalamia bavarica* (OTT 1967).**
Longitudinal section of a polyglomerate specimen. The good preservation of the sponge is the result of the Mg-calcitic mineralogy. The dark skeleton contrasts to the light-colored cements of the intraparticle pores, allowing skeletonization to be directly measured from microphotographs.
Sample HS6a; $\times 5$.
- Fig. 2: **Close-up view of *Alpinothalamia bavarica* with numerous chambers.**
The wall thickness of the different chambers varies considerably.
Sample HS6a; $\times 12$.
- Fig. 3: ***Uvanella? lamellata* SENOWBARI-DARYAN 1981.**
A common encruster of other reefbuilders. Some of the chambers exhibit vesiculae. *Uvanella* has a Mg-calcitic mineralogy and is, therefore, well-preserved.
Sample H9c; $\times 12$.
- Fig. 4: **Laser print of *Alpinothalamia bavarica* from Fig. 2.**
Even small details like vesiculae are well preserved.
Sample HS6a; $\times 11$.
- Fig. 5: **Laser print of *Uvanella lamellata* from Fig. 2.**
Vesiculae of the chamber and pores of the wall are visible.
Sample H9c; $\times 12$.
- Fig. 6: **Longitudinal section of *Alpinothalamia slovenica* (SENOWBARI-DARYAN 1982).**
This specimen has a similar skeletonization to that from Fig. 1.
Sample HS7b; $\times 8$.
- Fig. 7: **Laser print of a close-up view of *Alpinothalamia slovenica* from Fig. 9.**
Vesiculae are visible, filling the bubble-like chambers.
Sample HS7b; $\times 16$.
- Fig. 8: **Laser print of *Uvanella irregularis* OTT 1967 from Fig. 10.**
Sample L19b; $\times 8$.
- Fig. 9: **Close-up view of *Alpinothalamia slovenica* from Fig. 6.**
 $\times 18$.
- Fig. 10: **Microphotograph of *Uvanella irregularis*.**
In contrast to the specimen of Figs. 3 and 5, this specimen is weakly skeletonized.
 $\times 7$.

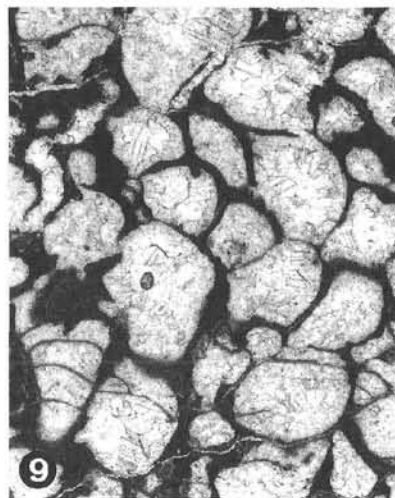
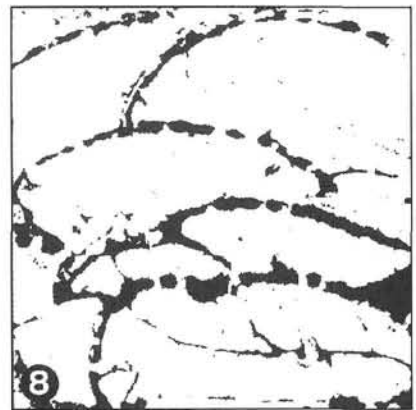
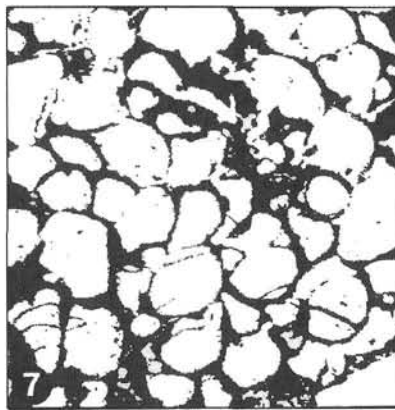
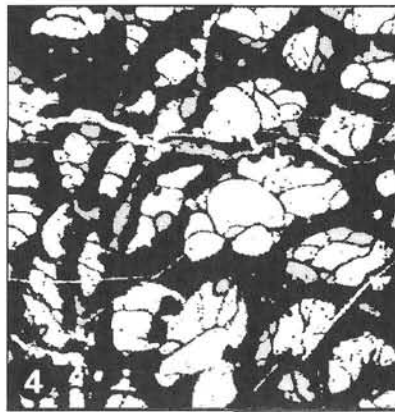
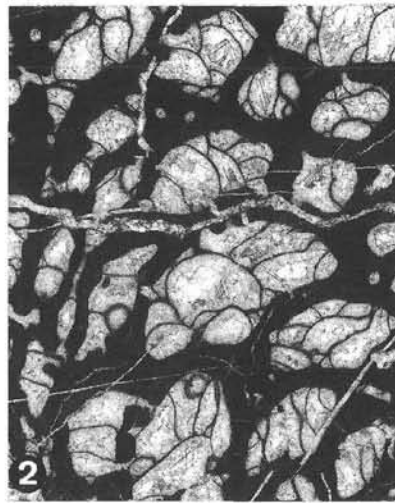
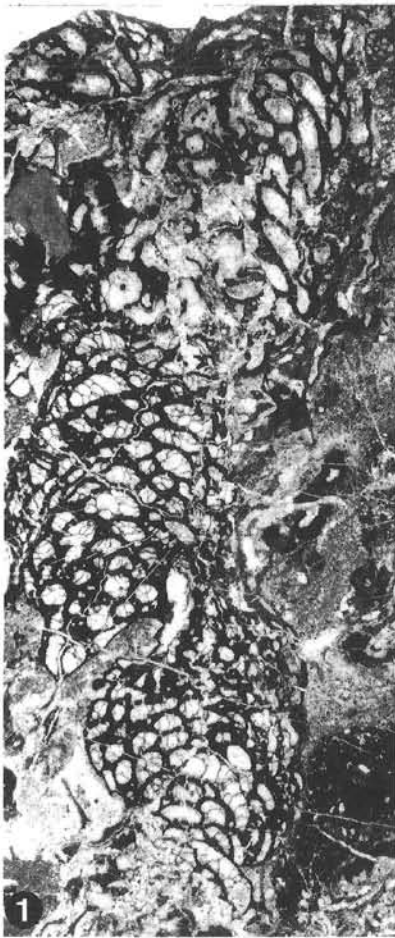


Plate 3

Microphotographs and laser prints of Upper Triassic inozoans and sphinctozoans.

- Fig. 1: **Upper Triassic inozoan (Inozoan gen. et sp. indet. 3).**
The sponge skeleton is characterized by a reticular structure and dichotomously branching canals.
Sample Wa 7; $\times 3.5$.
- Fig. 2: **Close-up view of the inozoan gen. et sp. indet. 3 illustrated in Fig. 1.**
Sample Wa 7; $\times 16$.
- Fig. 3: **Laser print of the inozoan illustrated in Fig. 1,2.**
Prior to dissolution of the metastable aragonite, sediment filled the intraparticle pores, sealing in the original thickness of the skeletal elements.
 $\times 15$.
- Fig. 4: **Longitudinal section of a globular colony of *Disjectopora* sp.**
Sample i 30; $\times 3$.
- Fig. 5: **Close-up view of another specimen of *Disjectopora* sp.**
Sample i 30; $\times 14$.
- Fig. 6: **Laser print of the specimen of *Disjectopora* sp. from Fig. 5.**
 $\times 13$.
- Fig. 7: **Longitudinal section of *Spongiomorpha ramosa* FRECH, 1890.**
Sample Wa 2b; $\times 2.5$.
- Fig. 8: **Close-up view of *Spongiomorpha ramosa* illustrated in Fig. 7.**
 $\times 12$.
- Fig. 9: **Laser print of another close-up view of the same specimen of *Spongiomorpha ramosa*.**
Sample Wa 2b; $\times 12$.

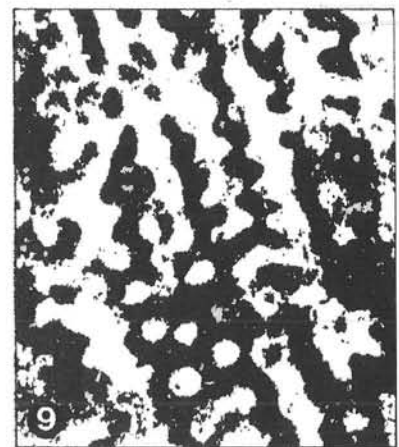
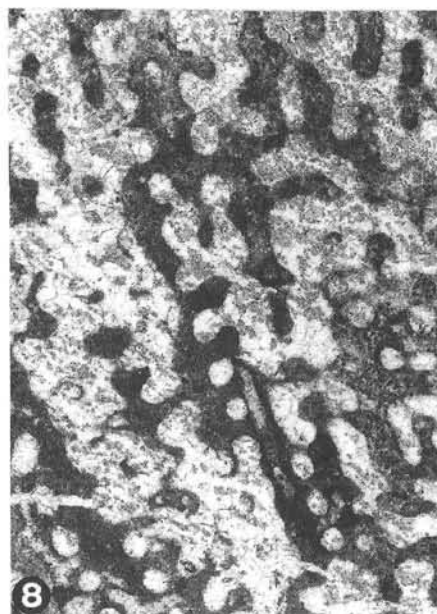
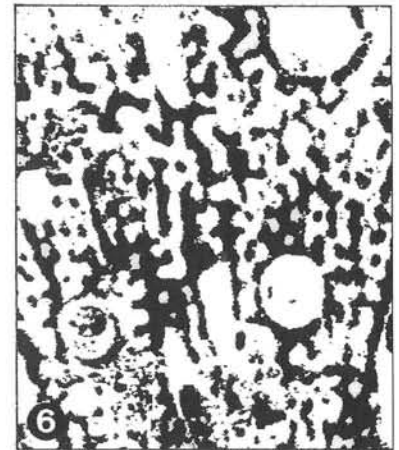
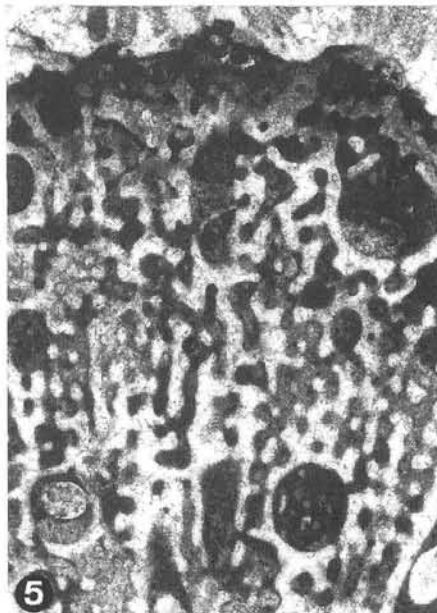
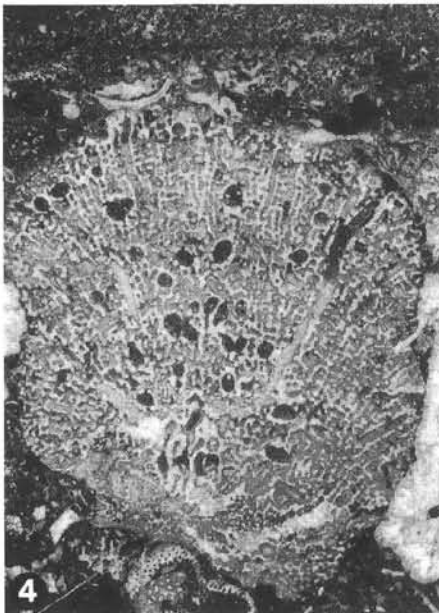
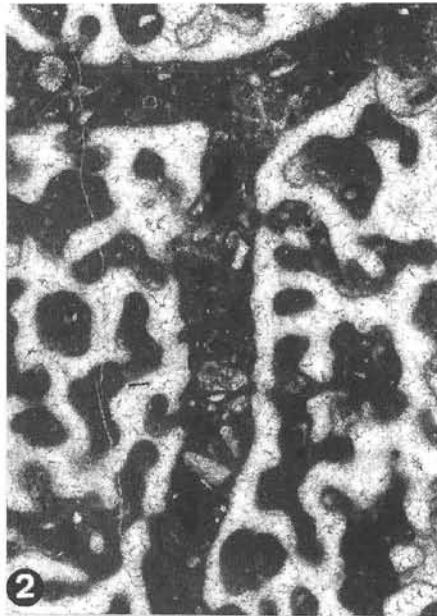
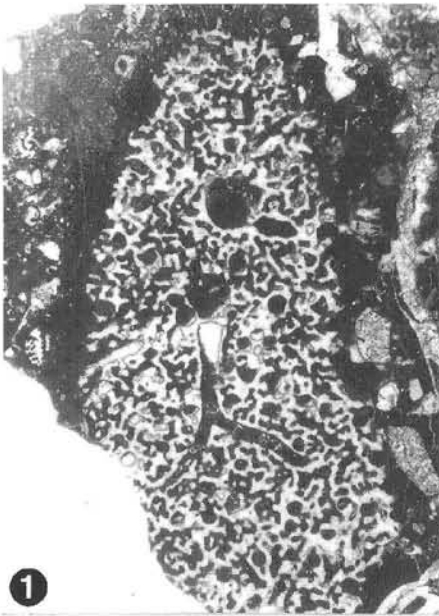


Plate 4

Microphotographs and laser prints of Upper Permian and Upper Triassic chaetetids and hydrozoans.

- Fig. 1: **Upper Triassic hydrozoan of Turkey.**
The original aragonitic skeleton is preserved.
Sample 19A1-2; $\times 4.5$.
- Fig. 2: **Close-up view of the hydrozoan illustrated in Fig. 1.**
 $\times 7.5$.
- Fig. 3: **Laser print of the hydrozoan illustrated in Fig. 1.**
 $\times 9.5$.
- Fig. 4: **Cross section of an Upper Permian chaetetid exhibiting the polygonal outline of the tubes.**
Sample SI; $\times 3.5$.
- Fig. 5: **Close-up view of the chaetetid illustrated in Fig. 4.**
 $\times 16$.
- Fig. 6: **Laser print of an Upper Triassic chaetetid with preserved aragonitic skeleton.**
Sample 19F33. $\times 6$.
- Fig. 7: **Laser print of the Upper Permian chaetetid from Figs. 4,5.**
 $\times 12$.
- Fig. 8: **Longitudinal section of the problematical Upper Permian hydrozoan *Pseudopalaeoaplysina* sp.**
Sample ZT 13; $\times 7$.
- Fig. 9: **Close-up view of *Pseudopalaeoaplysina* sp. illustrated in Fig. 8.**
 $\times 15$.

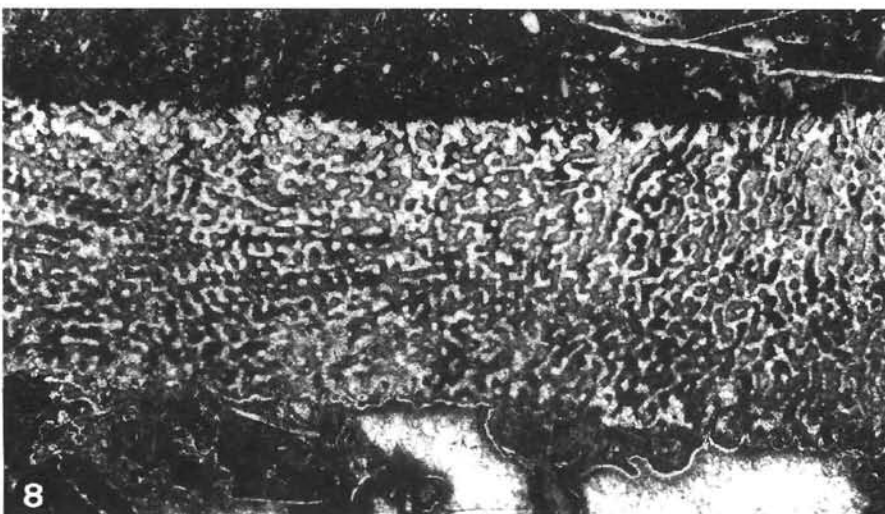
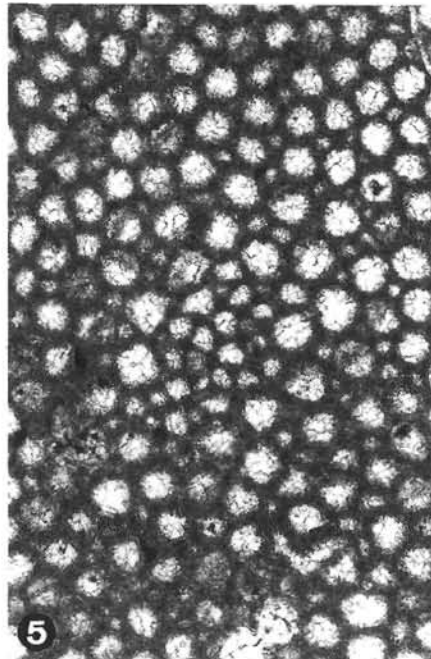
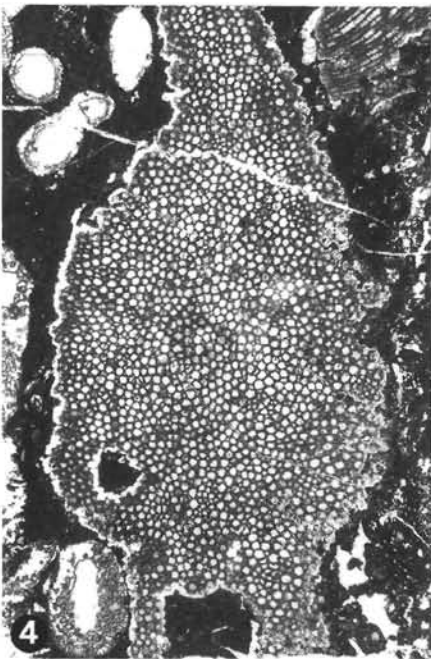
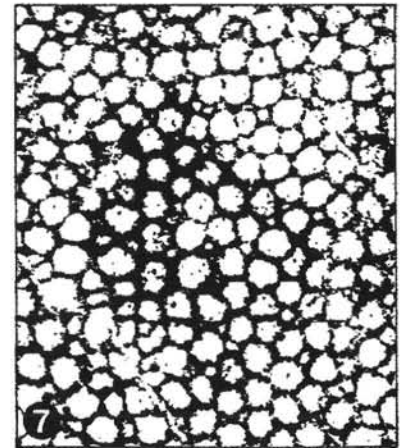
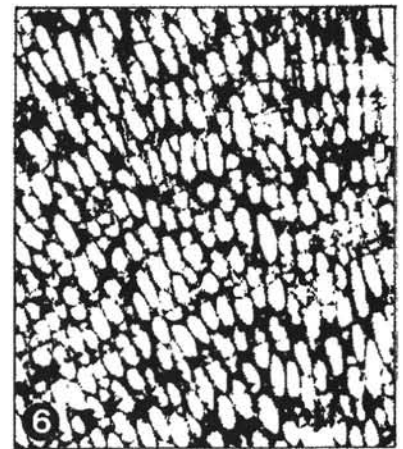
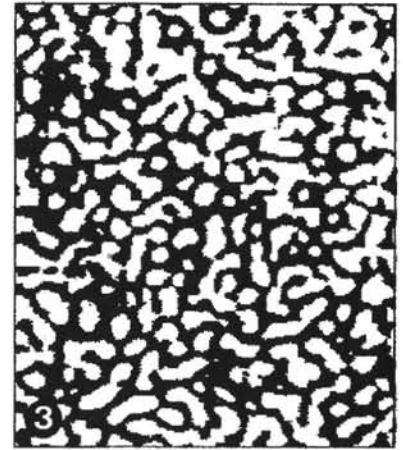
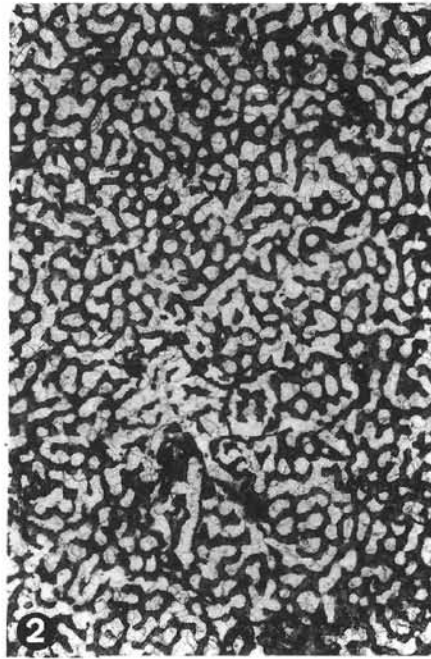
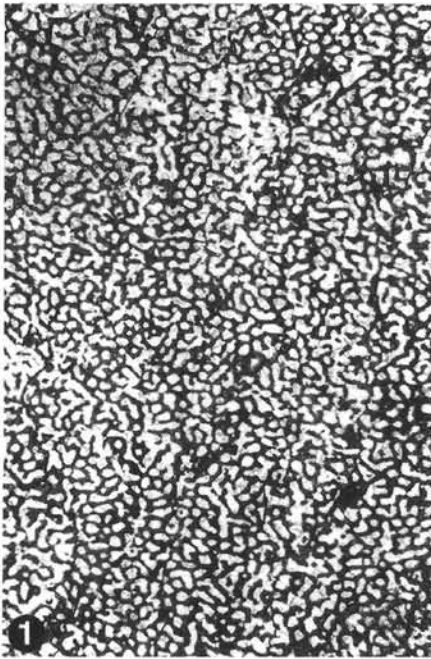


Plate 5

Microphotographs and laser prints of Upper Permian cerioid Rugosa.
The original microstructure of the investigated specimens is preserved.

- Fig. 1: **Cross section of *Wentzelella (Wentzelella) annae* (WAAGEN & WENTZEL 1886).**
Sample ZT 38; $\times 2.5$.
- Fig. 2: **Laser print of *Wentzelella (Wentzelella) annae*.**
Two complete calices were measured in this cross section.
Sample ZT 38; $\times 3$.
- Fig. 3: **Longitudinal section through *Wentzelella (Wentzelella) annae*.**
Distinct growth banding is visible.
Sample ZT 21; $\times 5$.
- Fig. 4: **Laser print of the longitudinal section from Fig. 3.**
Sample ZT 21; $\times 10$.
- Fig. 5: **Microphotograph of the calyx illustrated in Fig. 1.**
The original microstructure is clearly visible.
Sample ZT 43; $\times 16$.
- Fig. 6: **Laser print of a calyx of *Wentzelella (Wentzelella) wynnei* (BLENDINGER & H.W. FLÜGEL 1990) with columella and septa.**
Sample ZT43; $\times 16$.
- Fig. 7: **Laser print of the columella of *Wentzelella (Wentzelella) annae* shown in Fig. 1.**
Sample ZT 38; $\times 16$.
- Fig. 8: **Microphotograph of the wall of *Wentzelella (Wentzelella) wynnei*.**
Sample ZT 43; $\times 16$.
- Fig. 9: **Laser print of the wall and septa of *Wentzelella (Wentzelella) wynnei*.**
Sample ZT 43; $\times 16$.
- Fig. 10: **Laser print of the wall and septa of *Wentzelella (Wentzelella) annae*.**
Sample ZT 38; $\times 16$.

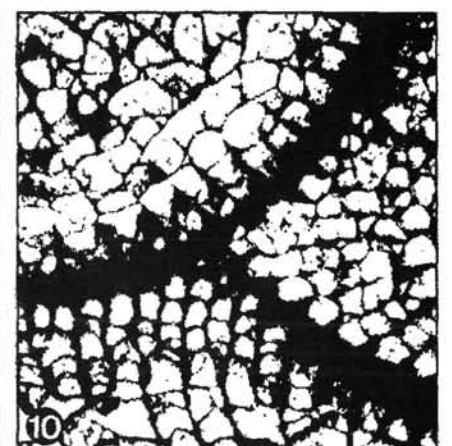
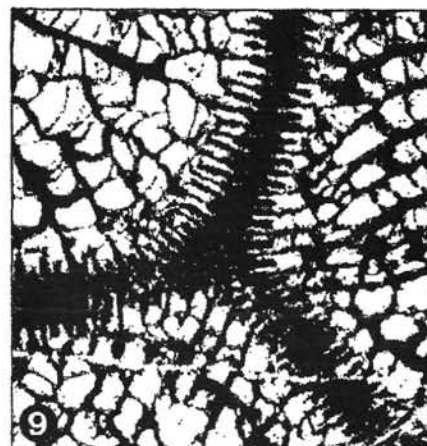
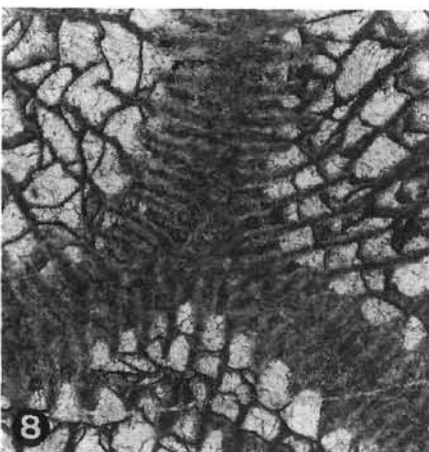
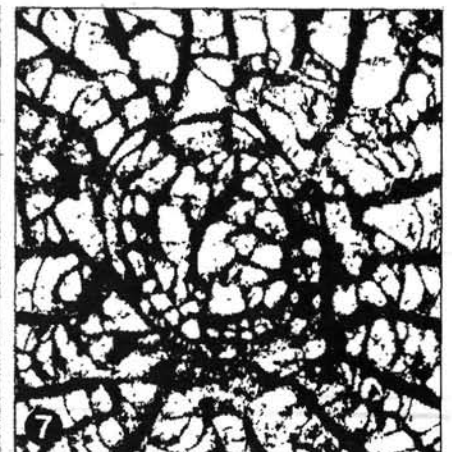
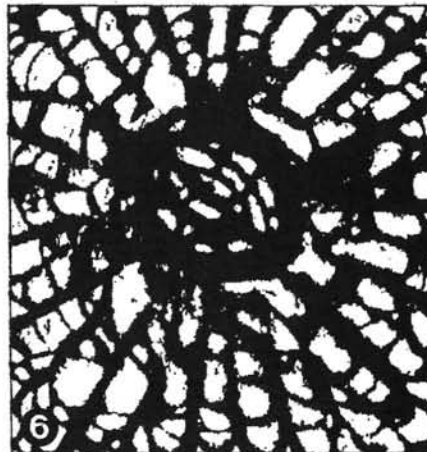
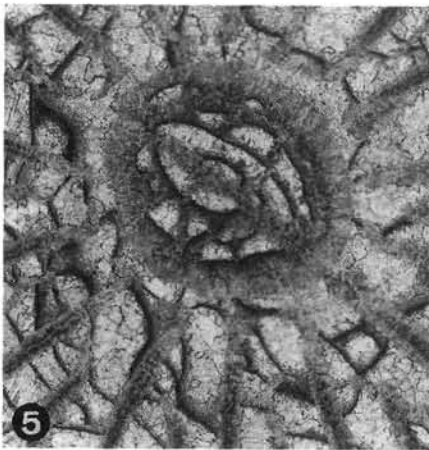
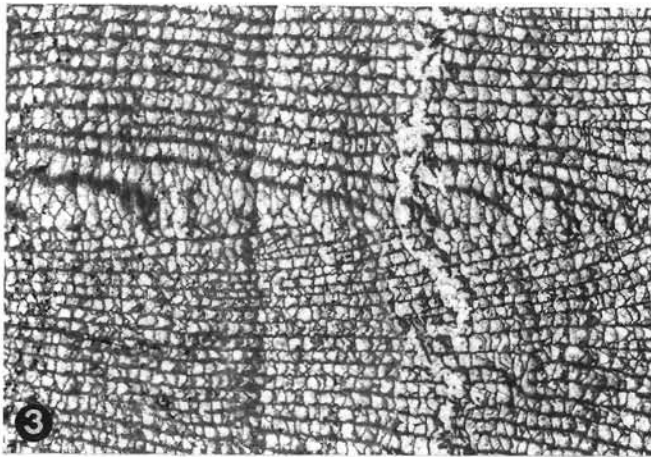
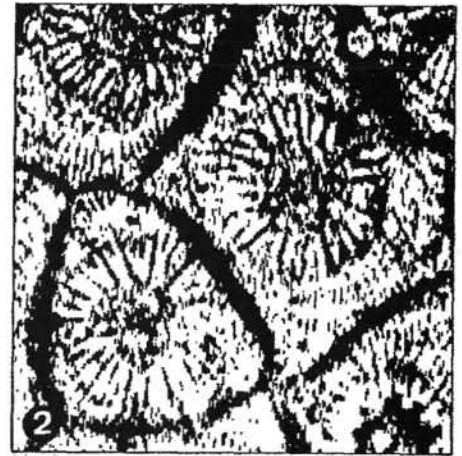
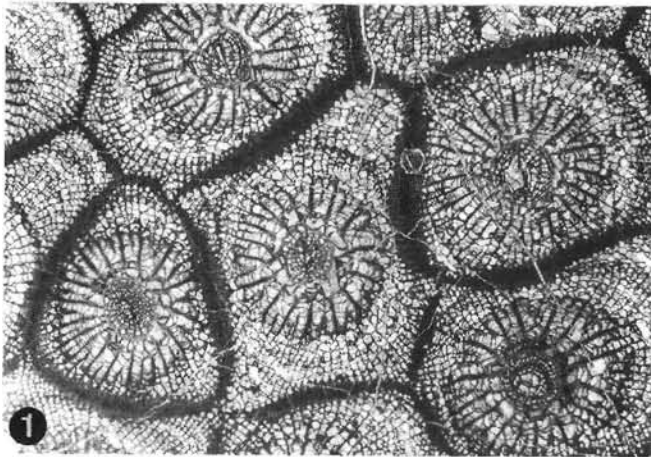
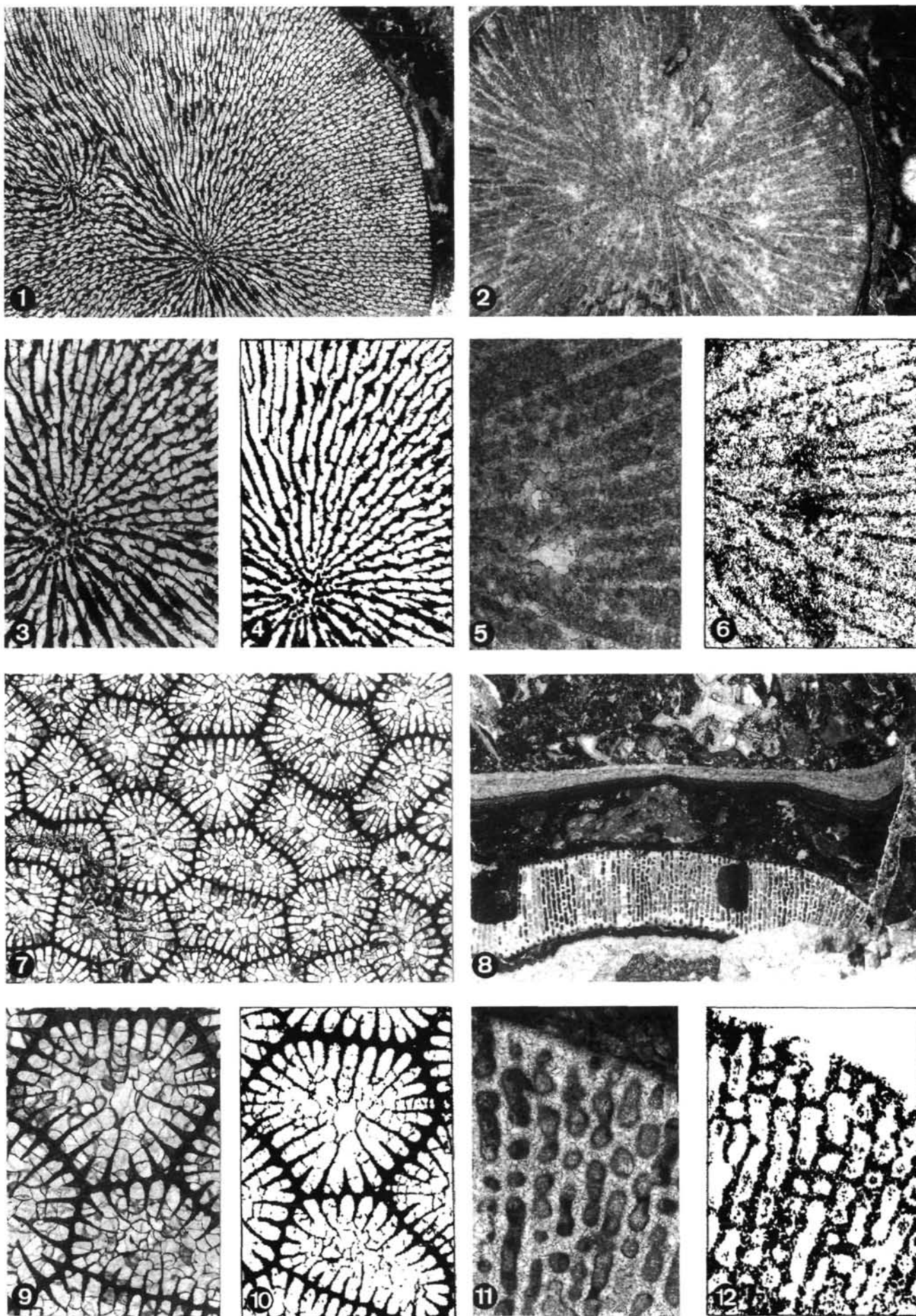


Plate 6

Microphotographs and laser prints of Upper Triassic scleractinians.

- Fig. 1: **Cross section of a *Montlivaltia*-type solitary coral with intratentacular budding.**
The original mineralogy is preserved. Skeleton and cement differ with respect to grey values.
Sample 19A11; $\times 2.5$.
- Fig. 2: **Cross section of a *Montlivaltia*-type solitary coral. Only relics of the skeletal elements can be observed as a result of recrystallization.**
The intraparticle pores are cemented instead of being filled with sediment. The contrast of cement and recrystallized skeleton is not distinct.
Sample JS1; $\times 2.5$.
- Fig. 3: **Close-up view of the specimen shown in Fig. 1.**
 $\times 5$.
- Fig. 4: **Laser print of the same specimen.**
 $\times 5$.
- Fig. 5: **Close-up view of the *Montlivaltia*-type solitary coral illustrated in Fig. 2.**
 $\times 6.5$.
- Fig. 6: **Laser print of the same specimen.**
 $\times 6.5$.
- Fig. 7: **Photomicrograph of the cerioid coral *Isastrea* sp. with preserved aragonitic skeleton.**
Sample 19A2; $\times 3$.
- Fig. 8: **Longitudinal section of the sheet-like coral *Seriastraea multiphylla* SCHÄFER & SENOWBARI-DARYAN 1978.**
The skeleton is converted into calcite. Sediment in the intraskeletal pores sealed in the original dimensions of the septa and dissepiments.
Sample KX4-1; $\times 2.5$.
- Fig. 9: **Cross section of *Isastrea* sp. with aragonitic skeleton.**
ample 19A2; $\times 5$.
- Fig. 10: **Laser print of the same specimen.**
 $\times 4.5$.
- Fig. 11: **Close-up view of the *Seriastraea multiphylla* SCHÄFER & SENOWBARI-DARYAN 1978.**
 $\times 14$.
- Fig. 12: **Laser print of the same specimen.**
 $\times 14$.



References

- BIRRARINI, F. & RUSSO, F. (1986): A new genus of inozoa from S. Cassiano Formation (Dolomiti Di Braies, Italy). – Mem. Scienze Geologiche, **38**, 129–135, 2 figs., 1 pl., Padova.
- BEURRIER, M., BÉCHENNEC, F., RABU, D. & HUTIN, G. (1986): Geological Map of Rustaq. Sheet NF 40–3D Scale 1 : 100.000. Explanatory notes. – Directorate General of Minerals, Oman Ministry of Petroleum and Minerals, Muscat.
- BLENDINGER, W. (1988): Permian to Jurassic deep water sediments of the eastern Oman Mountains: Their significance for the evolution of the Arabian margin of the South Tethys. – Facies, **19**, 1–32, 16 figs., 5 pls., Erlangen.
- BLENDINGER, W. & FLÜGEL H.W. (1990): Permische Stockkorallen aus dem Hawasina-Becken, Oman. – Facies, **2**, 139–146, 3 figs., 1 pl., Erlangen.
- BOSSCHER, H. (1992): Computerized tomography and skeletal density of coral skeletons. – Coral reefs, **12**, 97–103, 7 figs., 1 tab., Berlin.
- CREMER, H. (1993): Chaetetiden aus obertriassischen (Karn–Nor) Riffkalken der Westlichen Tauriden (Antalya-Region, SW Türkei): Morphologie, Systematik, Palökologie. – Unpubl. diploma thesis, Universität Erlangen, 102 p., 20 figs., 5 tabs., 16 pls., Erlangen.
- CUIF, J.P. (1972): Note sur les Madreporaires triasiques à fibres aragonitiques conservées. – C.R. Acad. Sci. (sér D), **277**, 2333–2336, 1 pl., Paris.
- DIECI, G., ANTONACI, A. & ZARDINI, R. (1968): Le spugne cassiane (Trias medio-superiore) della regione dolomitica attorno a Cortina d'Ampezzo. – Bull. Soc. Paleont. Ital., **7/2**, 94–155, 10 figs., pls. 18–33., Modena.
- DODGE R.E. & BRASS, G.W. (1984): Skeletal extension, density and calcification of the reef coral, *Montastrea annularis*: St. Croix, U.S. Virgin Islands. – Bull. Marine Science, **34**, 288–307, 4 figs., 6 tabs., Miami.
- FAGERSTROM, J.A. (1982): Stromatoporoids of the Detroit River Group and adjacent rocks (Devonian) in the vicinity of the Michigan basin. – Geol. Soc. Canada, Bull., **339**, 81 p. 33 figs., 8 pls., 8 tabs, Ottawa.
- FAGERSTROM, J.A. (1987): The Evolution of Reef Communities. – 600 p., 51 Taf., New York.
- FAGERSTROM, J.A. (1991): Reef-building guilds and a checklist for determining guild membership. – Coral Reefs, **10**, 47–52, 1 tab., Heidelberg.
- FAN, J., RIGBY, K.J. & WEI, Z. (1991): "Hydrozoa" from middle and upper Permian reefs of South China. – J. Paleont., **65/1**, 45–68, 17 figs., 7 tabs., Ithaca.
- FISCHER, J.C. (1970): Révision et essai de classification des Chaetetida (Cnidaria) post-paléozoïques. – Ann. Paléontol., **56/2**, 149–233, 35 figs., 6 pls., Paris.
- FLÜGEL, E. (1982): Microfacies analysis of limestones. – 633 p., 78 figs., 53 pls., 58 tabs., Berlin.
- FLÜGEL, E. & FLÜGEL-KAHLER, E. (1992): Phanerozoic Reef Evolution: Basic Questions and Data Base. – Facies, **26**, 167–278, 14 figs., Erlangen.
- FORSTER, A.B. (1985): Variation within coral colonies and its importance for interpreting fossil species. – J. Paleontol., **59**, 1359–1381, 8 figs., Tulsa.
- GLENNIE, K.W., BŒUF, M.G.A., HUGHES CLARKE, M.W., MOODY-STUART, M., PILAR, W.H.F. & REINHARDT, B.M. (1974): Geology of the Oman Mountains. – Verh. K. Ned. Geol. Mijnbouw. Genoot, **1/1–3**, Den Haag.
- HUTIN, G., BÉCHENNEC, F., BEURRIER, M. & RABU, D. (1986): Geological Map of Birkat al Mawz. Sheet NF 40–7B Scale 1 : 100.000. Explanatory notes. – Directorate General of Minerals, Oman Ministry of Petroleum and Minerals, Muscat.
- OEKENTORP, K. (1980): Aragonit und Diagenese bei permischen Korallen. – Münsterische Forschungen für Geologie und Paläontologie, **52**, 119–239, Münster.
- REITNER, J. (1992): Coralline Spongien – Der Versuch einer phylogenetisch-taxonomischen Analyse. – Berl. Geowiss. Abh., **E**, 352 p., 90 figs., 72 pls., Berlin.
- RIEDEL, P. (1990): Riffbiotope im Karn und Nor (Obertrias) der Tethys: Entwicklung, Einschnitte und Diversitätsmuster. – Unpubl. PhD thesis, Universität Erlangen, 96 p., 36 figs., 15 pls., 9 tabs., Erlangen.
- RIGBY, J.K., FAN, J. & ZHANG, W. (1989): Inozoa calcareous porifera from the Permian reefs of South China. – J. Paleont., **63/6**, 778–800, 13 figs., 6 tabs., Ithaca.
- RONIEWICZ, E. (1989): Triassic scleractinian corals of the Zlam-bach Beds, Northern Calcareous Alps, Austria. – Österr. Akad. Wiss., math.-naturwiss. Kl., Denkschriften, **126**, 1–152, 43 ps., 2 tabs, Wien.
- SEARLE, M.P. and GRAHAM, G.M. (1982): "Oman Exotics" – Oceanic carbonate build-ups associated with the early stages of continental rifting. – Geology, **10**, 43–49, 5 figs., Boulder.
- SENOWBARI-DARYAN, B. (1990): Die systematische Stellung der thalamiden Schwämme und ihre Bedeutung in der Erdgeschichte. – Münchner Geowiss. Abh., Reihe A, Geologie, **21**, 326 p., 70 figs., 63 pls., 18 tabs., München.
- SENOWBARI-DARYAN, B. (1991): "Sphinctozoa": an overview. – In: REITNER, J. & KEUPP, H. (Eds.), 224–241, 8 figs., Berlin.
- SENOWBARI-DARYAN, B. & RIGBY, J.K. (1988): Upper Permian Segmented Sponges from Djebel Tebaga, Tunisia. – Facies, **19**, 171–250, 15 figs., 19 pls., 4 tabs., Erlangen.
- SORAU, J.E. (1983): Primary biogenic structures and diagenetic history of Timorophyllum wanneri (Rugosa), Permian, Timor, Indonesia. – Mem. Ass. Australas. Palaeontols., **1**, 275–288, 9 figs.
- VILLEY, M., LE MÉTOUR, D. & DE GRAMONT, X. (1986): Geological map of Fanjah. Sheet NF 40–3F Scale 1 : 100.000. Explanatory notes. – Directorate General of Minerals, Oman Ministry of Petroleum and Minerals, 68 p., 16 figs., Muscat.
- WATTS, K.F. & GARRISON, R.E. (1986): Sumeini Group, Oman–Evolution of a Mesozoic carbonate slope on a south tethyan continental margin. – Sed. Geol., **48**, 107–168, 26 figs., 1 tab., Amsterdam.
- WENDT, J. (1990): The first aragonitic rugose coral. – J. Paleont., **64/3**, 335–340, 2 figs., 1 tab., Lawrence.

ZOBODAT - www.zobodat.at

Zoologisch-Botanische Datenbank/Zoological-Botanical Database

Digitale Literatur/Digital Literature

Zeitschrift/Journal: [Abhandlungen der Geologischen Bundesanstalt in Wien](#)

Jahr/Year: 1994

Band/Volume: [50](#)

Autor(en)/Author(s): Bernecker Michaela, Weidlich Oliver

Artikel/Article: [Attempted Reconstruction of Permian and Triassic Skeletonization from Reefbuilders \(Oman, Turkey\): Quantitative Assessment with Digital Image Analysis 31-56](#)